



Flood hazard in tourism development area Gunjur, the Gambia

**Mapping and exploring mitigation strategies
using UAV methodology**



BSc thesis by Nik Verweel

July 2023

**Soil Physics and
Land Management Group**

 WAGENINGEN UNIVERSITY
WAGENINGEN UR

Flood hazard in tourism development area Gunjur, the Gambia Mapping and exploring mitigation strategies using UAV methodology

Bachelor thesis Soil Physics and Land Management Group
submitted in partial fulfilment of the degree of Bachelor of Science
in International Land and Water Management at Wageningen
University, the Netherlands

Study program:
BSc International Land and Water Management

Student registration number:
1012884

YWU 80812

Supervisors:
WU supervisor: Teun Vogel, MSc.
Host supervisors: Wilma Dijkstra & Martin Breedveld

Examinator:
Prof. Coen Ritsema

Date:
14/07/2023

Soil Physics and Land Management Group, Wageningen University

Abstract

The increasing pressures of climate change in combination with a history of sand excavation have left stretches of the Gambian coastline vulnerable to coastal and terrestrial flooding. At the same time, in a bid to revitalise and encourage tourism, the Gambian government has allocated some of these stretches of coast as Tourism Development Area. During this study, a combined UAV methodology was used to map the coastal flooding vulnerability and terrestrial flood hazard, in order to recommend mitigation strategies to be considered during tourism development projects near Gunjur. The coastal flooding vulnerability was found to be very high, the terrestrial flood hazard was found to be predominantly high or very high, and the dune system was found to be susceptible to erosion and potential failing. This study highlights the need for mitigation measures aimed at coastal defence and precipitation interception, not just to benefit the sustainable development of tourism destinations near Gunjur, but potentially for the wider Gambian coastline.

Table of Contents

1	Introduction.....	1
1.1	General Introduction.....	1
1.2	Research Objective and Research Questions	3
2	Method and Materials.....	4
2.1	Methodology	4
2.1.1	UAV Imagery Collection and Ground Control Points	5
2.1.2	Digital Terrain Model and Orthorectified Image	5
2.1.3	Coastal Vulnerability Index	6
2.1.4	Terrestrial Flood Hazard	7
2.1.5	Dune Survey	8
2.1.6	Mitigation Strategies.....	9
2.2	Materials	9
3	Results.....	10
3.1	Base results.....	10
3.2	Coastal Vulnerability Index (SRQ1).....	10
3.3	Terrestrial Flood Hazard (SRQ2).....	11
3.4	Dune Survey (SRQ3)	12
3.5	Mitigation Strategies (SRQ4)	15
3.5.1	Strategies aimed at reducing coastal vulnerability	15
3.5.2	Strategies aimed at reducing terrestrial flood hazard	16
3.5.3	Strategies aimed at improving dune structure.....	17
4	Discussion	19
4.1	Discussion of Results and Methodology	19
4.1.1	Coastal Vulnerability Index	19
4.1.2	Terrestrial Flood Hazard	19
4.1.3	Dune Survey	20
4.2	Validity and Reliability.....	21
4.2.1	Validity	21
4.2.2	Reliability	21
5	Conclusion.....	23
5.1	General Conclusion.....	23
5.2	Recommendations	23
References	25	
Annexes	30	
Annex I	30	
Annex II	31	
Annex III.....	34	
Annex IV	37	
Annex V	40	
Annex VI	42	

Annex VII	43
Annex VIII	44
Annex IX	45
Annex X	46

Table of Figures

Figure 1 - Reference map of the study area	2
Figure 2 - Data action model to accompany methodology.	4
Figure 3 - Visualisation of terrestrial flood hazard.	11
Figure 4 - Visualisation of dune vegetation classification.	13
Figure 5 - Visualisation of dune slope classification.	13
Figure 6 - Bivariate visualisation of dune survey results.	14
Figure 7 - Visualisation of suitable locations for discussed intervention strategies.	18

Table of Tables

Table 1 - Variables of the Coastal Vulnerability Index.....	6
Table 2 - Relative sea lever rise rate per RCP scenario.	7
Table 3 - Overview of collected satellite imagery.....	7
Table 4 – Overview of flood hazard factors	8
Table 5 - Classification of slope for bivariate visualisation.	9
Table 6 - Results for each variable of the CVI calculation.	10
Table 7 - Results from in-field dune survey.....	12
Table 8 - Results of supervised classification of dune areas.....	12
Table 9 - Results of species identification and frequency during dune survey.....	14
Table 10 - Overview of possible mitigation strategies.	15

1 Introduction

1.1 General Introduction

It is no news that the global climate is changing. Research has strongly suggested a link between humans and climate change (Wuebbles et al., 2017), and the effects of the global climate being influenced at an unprecedented level by human activities (*Consequences of Climate Change*, n.d.). Relationships between the changing environment and global climate systems have been researched extensively. It is thought that processes like the rising of global sea levels (IPCC, 2023) and the increasing severity and frequency of weather extremes (Herring et al., 2022) are partially caused by the changing climate. With the changing of these global climate systems, an increase in climate-related disasters such as floods and wildfires has been observed (Diaconu et al., 2021; Tyukavina et al., 2022), with models showing it is likely the frequency will only increase further (Hirabayashi et al., 2021).

Flooding in particular is expected to be a problematic issue in the coming decades, with up to 45% of the human population living in coastal communities (Bosch et al., 2010). It is no wonder then, that flooding is discussed at length in climate change-related literature, spanning from scientific research to policy reports such as the 2021 IPCC report (IPCC, 2021).

As the global scientific community has become aware of the effects of climate change on flood frequency, different methods of mapping flood risk, hazard and vulnerability have been developed (Diaconu et al., 2021). Flood hazard (the probability of occurrence of a potentially damaging flood event), flood vulnerability (the degree of loss resulting from the occurrence of the flood event) and flood risk (the combination of hazard and vulnerability), are increasingly being mapped using geo-information systems (GIS) methodologies. Within the GIS domain, multiple methodologies have been developed differentiating between terrestrial (inland) flood risk and coastal flood risk. Research by Diaconu et al. (2021) shows that the most popular methodologies within the GIS domain are modelling/simulation and statistical analysis, with 24% and 20% of papers published between 1979 and 2020 belonging to these methodologies respectively. Combined (a mix of several methodologies) and remote sensing methodologies represent 16% and 8% of the published articles, respectively.

Within the remote sensing domain, a relatively new field utilising Unmanned Aerial Vehicles (UAVs, commonly known as drones) is emerging. The higher spatial resolution of UAV imagery compared to traditional (open access) remote sensing data offers mapping in higher detail, but usually on a smaller scale. The high spatial resolution and accuracy of UAV imagery, compared against typical remote sensing data sources, has shown promise in the generation of detailed orthorectified (mosaic) imagery and Digital Elevation Models, and also for flood hazard mapping applications (Annis et al., 2020; Iizuka et al., 2018). Higher resolution imagery may also logically lead to the opportunity to design more bespoke intervention plans and management structures, as algorithms and models also achieve higher accuracies when compared against other types of remote sensing data such as satellite imagery. However, research on the use of UAV imagery in the flood mapping and mitigation domain is still limited.

While the changing climate is putting pressures on global shorelines and increasing the frequency and severity of floods, the government of the Gambia has allowed the excavation of coastal zones behind naturally occurring dunes as a source of sand to be used in the construction materials industry and as an export good. The government describes the excavation efforts to "be a key to our [the Gambian] economic development" (*Mining and Quarrying - MoPE, the Gambia*, n.d.). Though initially at a limited volume and dependant on contracts and permits, some areas have been excavated beyond the agreed upon volume through illegal excavation. Gambian newspapers and online reports are filled with the extent and issues arising from the (illegal) excavation, with it being described as "a major crisis" (*The Effects of Sand Mining*, 2022), "in violation of environmental laws" (*Sand Mining: Gambia's Miss-opportunities – Know Your Budget*, n.d.) and noting "it can cause disaster in the future" (Jadama, 2021). As a result of the excavation practises, stretches of the already vulnerable Gambian coast lay bare and have become even more vulnerable.

In a bid to revitalise the tourism industry in the Gambia after decreasing tourist numbers due to global factors such as the Ebola scare and more recently the Covid-19 pandemic (Ayeni, 2020; *Development and Importance of Tourism for Gambia*, n.d.; Novelli et al., 2018), the Gambia Tourism Board (GTB) has announced plans to develop new tourism destinations along the coastline, called Tourism Development Areas (TDAs). One such TDA is found near Gunjur town in the Western Division in the Gambia (Figure 1), an area previously used for sand excavation. The GTB now requests private investors to submit plans for these TDAs, but concerns are being raised by developers regarding the sustainability of such a project due to the aforementioned climate concerns. As especially coastal areas have been found to be at risk of the changing climate, it appears a high-risk venture for project developers, as flooding can cause considerable damage to the proposed projects.

Reference map of study area

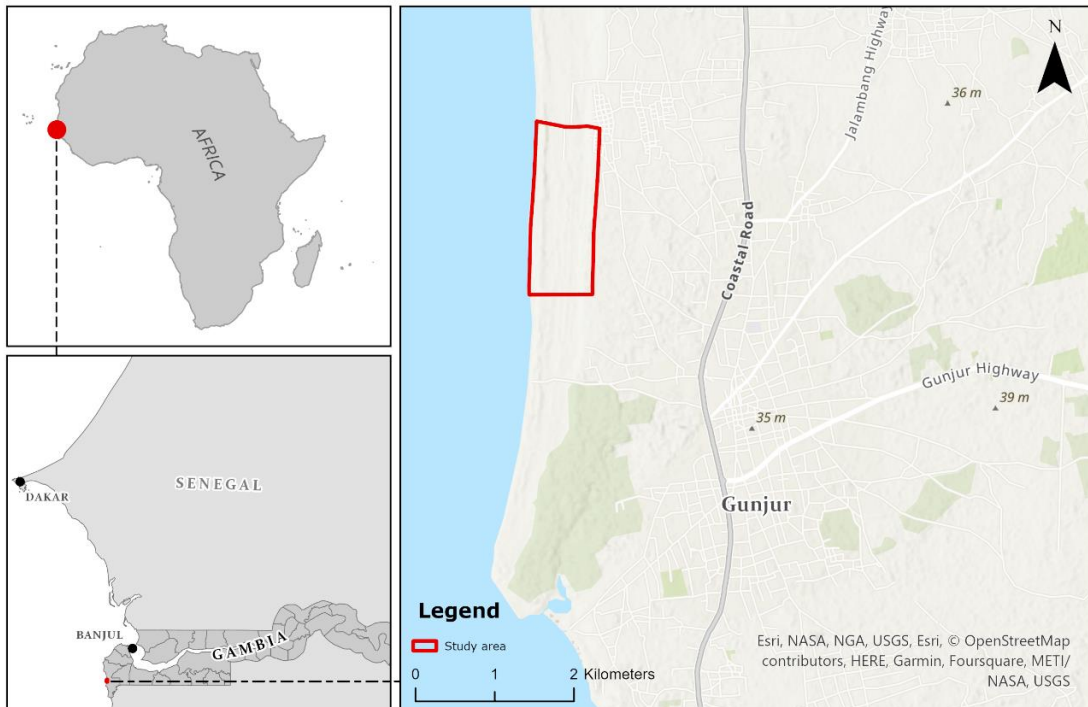


Figure 1 - Reference map of the study area. (Source: author)

The combination of the changing climate and recent coastal management present a problem, as the coastal area not just near Gunjur, but along the Gambian coast, will have to show resilience against climate challenges whilst in a relatively poor state. On top of this, the broader Gambian coastline is to be developed into tourism destinations, whilst little to no attention is being paid to the aforementioned problems. Further contributing to this issue is the uncertainty, as it is not yet exactly clear to what extent the aforementioned issues are grounded with scientific proof, and which issues should take priority for potential project developers.

1.2 Research Objective and Research Questions

Considering the issues at play, the objective of this thesis is to determine the coastal flooding vulnerability and terrestrial flood hazard of the TDA in Gunjur, the Gambia, through the application of known methodologies in combination with novel data collection methods. Based on the findings of the research, a combination of interventions will be suggested to reduce the vulnerability and hazard to allow more sustainable development of tourism destinations in the outlined area.

In order to successfully complete the research objective, the following general research question is defined:

"What level of coastal flooding vulnerability and terrestrial flood hazard are present at the tourism development area near Gunjur, Gambia, and what are options for mitigation to guarantee sustainable tourism development?"

This general research question is further divided into several specific research questions (SRQs) that combine to answer the general research question:

SRQ1: What is the level of coastal vulnerability, expressed in the Coastal Vulnerability Index (CVI), in the tourism development area?

SRQ2: What is the level of terrestrial flood hazard in the tourism development area?

SRQ3: What is the state of the dunes within the tourism development area?

SRQ4: What are potential options for decreasing coastal flood vulnerability and mitigating terrestrial flood hazard?

2 Method and Materials

2.1 Methodology

The research questions outlined in the previous section will be answered by combining multiple methodologies that have been previously applied in scientific literature, in combination with a novel method of data collection.

Figure 2 shows the Data Action Model for all data collected and the subsequent data processing steps.

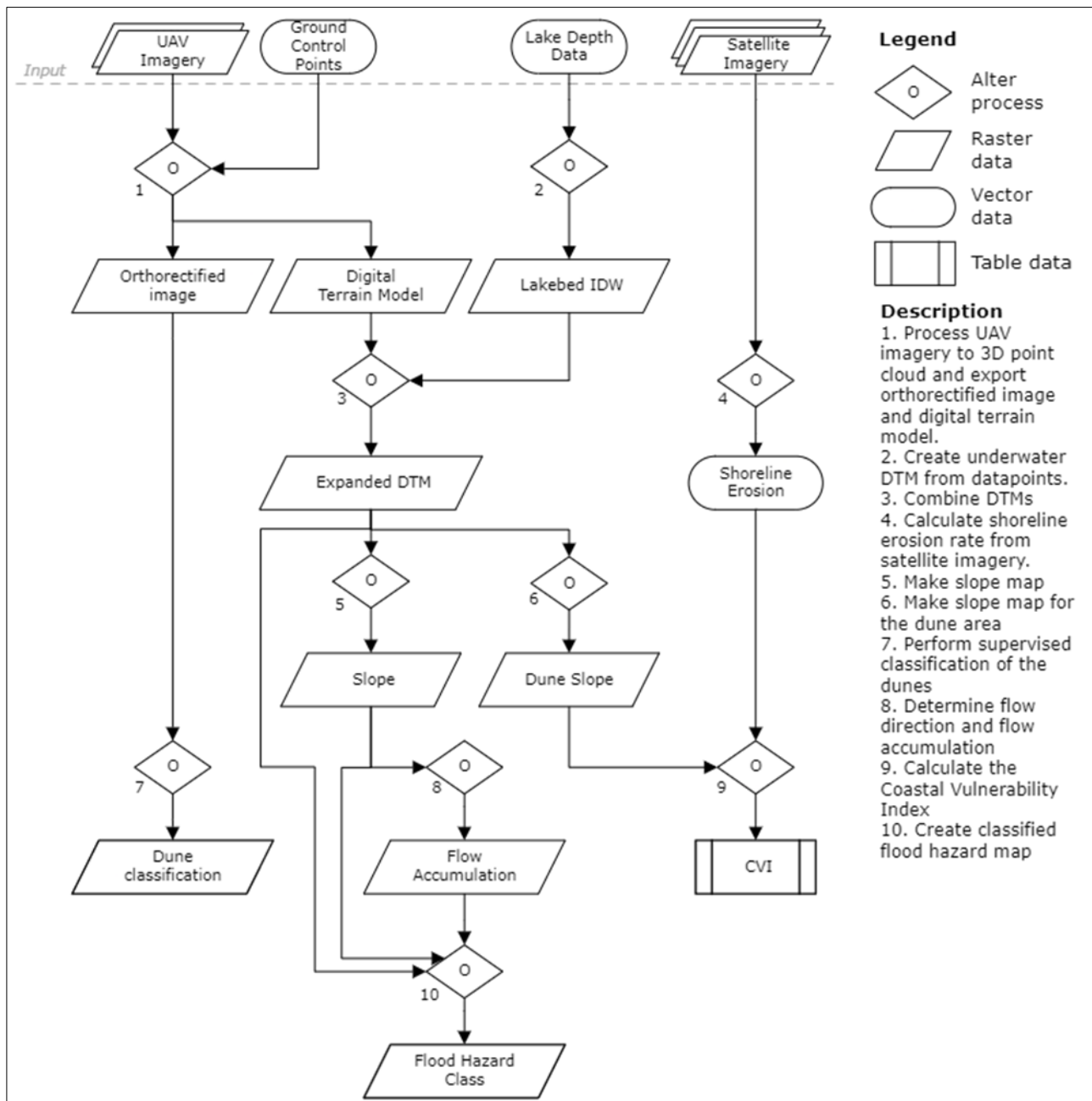


Figure 2 - Data action model to accompany methodology.

Within the ArcGIS Pro environment, the tools used were divided into several phases and processed through the use of models, for reproducibility. These models can be found in Annex I through Annex V.

2.1.1 UAV Imagery Collection and Ground Control Points

Central to the methodology, as source for multiple products used in various SRQs, was the collection of the UAV imagery. The imagery was collected using a DJI Mavic Pro 1, outfitted with a GPS and 12MP camera quality. The drone was flown at an altitude of 120 m, resulting in a ground spatial resolution of ~0.07 m. The project area was divided into several sub areas to facilitate the data collection missions, each spanning roughly 17.5 hectares (ha). At the time of data collection, some 66.5 ha of the project area was under water. This area was left out from the imagery collection mission as it could not be used towards the end products, as it would appear as a flat surface when converted into a 3D environment. In total this left around 105.3 ha of the study area being imaged. Images were verified after the mission to check whether overlap between images was achieved and whether there were any errors (blurriness, artefacts) in the images.

To facilitate the processing of the UAV imagery to a 3D geo-referenced point cloud, Ground Control Points (GCPs) were collected. Twelve GCPs were collected at locations where a landmark was likely to be visible on the UAV imagery using a Trimble DA2 Catalyst GNSS System (Annex VI). At each location, the GCP was collected with a vertical and horizontal accuracy below 5 cm. The GCPs were collected in a zig-zag pattern across the project area, ensuring that the whole project area was accurately represented in 3D.

2.1.2 Digital Terrain Model and Orthorectified Image

The results for SRQ1, SRQ2 and SRQ3 all include a product from the collected UAV imagery, in either the form of a Digital Terrain Model (DTM) or an orthorectified image. These products were realised through a workflow in Agisoft MetaShape, a software programme for processing 3D point clouds.

The generation of the 3D point cloud from the UAV imagery in Agisoft MetaShape was achieved by aligning all the UAV imagery in high-quality and inputting the GCP markers. Through the alignment of the UAV imagery to the GCP markers, the 3D point cloud was georeferenced, after which a processing report was generated. Subsequently, a dense point cloud was generated in colour with mild depth filtering. A first pass of manual filtering was conducted to remove some areas of the dense cloud that should not have been included, like reed areas surrounding the lake banks. After this, the orthorectified image was exported to ArcGIS Pro.

To further process the dense cloud into a suitable DTM, a classification was performed to find only the ground surface, with other objects like trees and buildings abstracted. This was done using the Classify Ground Points with a confidence rate of 0.5, as higher confidences (>0.5) were found to result in high levels of misclassification in preliminary research. The classified dense cloud of ground points was exported as base DTM into ArcGIS Pro to allow the addition of height data for the area under water, which was left out of the UAV imagery collection as described in section 2.1.1.

Depth data for the underwater area were collected in two phases. First, 56 depth measurements were collected around the banks of the lake using a measuring stick, which were linked to GPS data collected through a smartphone application, with an accuracy of at least 5 m. Secondly, 17 depth measurements were taken further into the lake using a rowing boat, measuring stick and Trimble DA2 Catalyst GNSS System to georeferenced the depth measurement with an accuracy of at least 30 cm. Subsequently, these point datasets were combined in ArcGIS Pro and processed into a depth map of the lake through Inverse Distance Weighted (IDW) Interpolation with power 2 and 15 used points. The resolution of the IDW raster was set to the same size as the previously generated DTM from Agisoft MetaShape (0.07 m). The Agisoft MetaShape DTM and IDW lake depth map were combined through raster mosaicking to create a single raster dataset containing the DTM for the study area, enriched with depth data for the lake.

The DTM was resampled in ArcGIS Pro using Bilinear Interpolation to a resolution of 1 m. This was necessary as running several of the modelling tools in ArcGIS Pro produced incorrect results when using the DTM at 0.07 m resolution.

2.1.3 Coastal Vulnerability Index

To calculate the Coastal Vulnerability Index, a known methodology developed by the United States Geological Survey (USGS), was applied (USGS, n.d.). This methodology ranks six variables contributing to coastal vulnerability on a scale between very low and very high, as shown in Table 1.

Table 1 - Variables of the Coastal Vulnerability Index (USGS, n.d.).

Variable	Ranking of coastal vulnerability index				
	Very low 1	Low 2	Moderate 3	High 4	Very high 5
Geomorphology, <i>a</i>	Rocky, clifffed coasts, fiords, fiards	Medium cliffs, indented coasts	Low cliffs, glacial drift, alluvial plains	Cobble beaches, estuary, lagoon	Barrier beaches, sand beaches, salt marsh, deltas, mangrove
Coastal slope, <i>b</i> (%)	> 0.2	0.2 - 0.07	0.07 – 0.04	0.04 – 0.025	< 0.025
Relative sea-level change, <i>c</i> (mm/y)	< 1.8	1.8 – 2.5	2.5 – 2.95	2.95 – 3.16	> 3.16
Shoreline erosion / accretion, <i>d</i> (m/y)	> 2.0	1.0 – 2.0	+1.0 – -1.0	-1.1 – -2.0	< -2.0
Mean tide range, <i>e</i> (m)	> 6.0	4.1 – 6.0	2.0 – 4.0	1.0 – 1.9	< 1.0
Mean wave height, <i>f</i> (m)	< 0.55	0.55 - 0.85	0.85 – 1.05	1.05 – 1.25	> 1.25

The CVI is subsequently calculated using Equation 1 as shown below.

$$CVI = \sqrt{((a * b * c * d * e * f) / 6)} \quad (Equation\ 1)$$

To calculate each variable of the CVI, varying methodologies were applied. The geomorphology variable was defined through visual identification.

The coastal slope variable was calculated using the 1 m DTM, explained in section 2.1.2, though clipped to only include the beach area. The slope was calculated in the ArcGIS Pro environment (in %), with the z-factor set to 1. Subsequently, the coastal slope map was reclassified into the CVI index classification shown in Table 1 for further use in the CVI calculation.

To ensure relevance to future climatic conditions, projected values for the relative sea-level change variable were used, calculated using data relevant to the Gambian coast, retrieved from the World Bank's Climate Change Knowledge Portal (World Bank, n.d.). The relative sea-level rise rate was calculated for three Representative Concentration Pathway (RCP) projections (RCP2.6, RCP4.5, and RCP8.5) using Equation 2:

$$\text{Relative sea level rise rate, } c \left(\frac{\text{mm}}{\text{yr}} \right) = \frac{MPSLR_{48} - MPSLR_{23}}{25} * 1000 \quad (Equation\ 2)$$

Where,

$MPSLR_{48}$ = Median Projected Sea Level Rise 2048

$MPSLR_{23}$ = Median Projected Sea Level Rise 2023

Based on the different RCP scenarios, the three different rates of relative sea level rise are found below in Table 2 (next page).

Table 2 - Relative sea lever rise rate, c , per RCP scenario.

RCP Scenario	Median Projected Sea Level Rise 2023 (m)	Median Projected Sea Level Rise 2048 (m)	Relative sea level rise rate, c (mm/y)
RCP 2.6	0.11	0.22	4.4
RCP 4.5	0.10	0.23	5.2
RCP 8.5	0.10	0.26	6.4

The rate of shoreline erosion / accretion was calculated by applying a simple version of shoreline digitization methodology, in which the shorelines are estimated using satellite imagery on a visual basis. More sophisticated models were considered but could not be achieved due to time constraints. Based on historical satellite imagery of the study area, presented in Table 3 with their respective acquisition date and spatial resolution, the shorelines were drawn in in ArcGIS Pro. Pre-processing was not required as the data acquired was already a Data Processing Level 2 product, meaning it is ready for use straight away (Blumenfeld, 2021). Subsequently, points were drawn along each individual digitised shoreline in increments of 5 m, which was used as input for the Near tool. This generated an overview of the difference in distance between the points for each specific year, allowing for the calculation of the rate of shoreline erosion / accretion for each time step and for as a whole.

Table 3 - Overview of collected satellite imagery. Landsat imagery acquired through USGS EarthExplorer (United States Geological Survey, n.d.), Sentinel imagery acquired through ESA's Copernicus Hub (European Space Agency [ESA], n.d.).

Platform	Date	Bands	Spatial resolution
Landsat 7	February 19 th 2010	Red, Green, Blue	30 m
Landsat 7	February 25 th 2012	Red, Green, Blue	30 m
Landsat 8	February 22 nd 2014	Red, Green, Blue	30 m
Sentinel 2	February 3 rd 2016	Red, Green, Blue	10 m
Sentinel 2	February 22 nd 2018	Red, Green, Blue	10 m
Sentinel 2	February 27 th 2020	Red, Green, Blue	10 m
Sentinel 2	February 26 th 2022	Red, Green, Blue	10 m

The mean tidal range and mean wave height were both calculated through averaging the tide range and wave height respectively from using tidal data acquired online from the Bakau tide station, some 40 km further up the coast (*Tide Table for Bakau*, n.d.). The Department of Water Resources was approached for this data, though they did not provide it. The data available online consisted of a 7-day tide forecast, showing high tide, low tide, and wave height. The mean tidal range was taken as the 7-day average of the difference between high and low tide. The mean wave height was taken as the 7-day average of the wave height.

2.1.4 Terrestrial Flood Hazard

The terrestrial flood hazard was quantified and mapped by applying and adjusting a methodology found in Kourgialas and Karatzas (2011), in which a Weighted Linear Combination (WLC) method is utilized to combine several factors to produce a classified hazard level. Due to the difference in scale between this research and the research by Kourgialas and Karatzas, several hazard factors were left out of the calculations. The land use, rainfall intensity and geology factors were excluded, as these are all fairly homogeneous in the research area.

The remaining factors, shown in Table 4, were calculated based on a resampled version of the DTM created in section 2.1.2.

The elevation factor was taken to be the value of the DTM, the slope factor was calculated using the Slope tool, and the flow accumulation factor was calculated by running the Flow Direction tool (using the D8 modelling algorithm) on the slope map, and subsequently running the Flow Accumulation tool. Each factor was classified into five classes, corresponding to the flood hazard level, using Natural Jenks. This resulted in the weighted factors as shown in Table 4 (next page).

Factors were combined through a Raster Calculator. For each cell, the combined hazard class was calculated as the weight of the effect (a) times the percentage of the sum of the weighted rating. The results were then classified back into the five flood hazard classes.

Table 4 – Overview of flood hazard factors with the associated weighted ratings and domains of effect, adapted from Kourgialas and Karatzas (2011).

Factor	Domain of effect	Flood hazard class	Weight of effect (a)	Rate (b)	Weighted rating ($a * b$)	Total weight	Percentage of sum (%)
Flow accumulation (pixels)	45090 - 10609	Very high	10	1.5	15.0	39	18.75
	10608 - 4420	High	8		12.0		
	4419 - 1945	Moderate	5		7.5		
	1944 - 530	Low	2		3.0		
	529 - 0	Very low	1		1.5		
Slope (degrees)	0 - 3.5	Very high	10	2	20.0	52	25
	3.6 - 10.5	High	8		16.0		
	10.6 - 20.6	Moderate	5		10.0		
	20.7 - 35.3	Low	2		4.0		
	35.4 - 81.0	Very low	1		2.0		
Elevation (m)	-1 - 2.1	Very high	10	4.5	45.0	117	56.25
	2.2 - 5.4	High	8		36.0		
	5.5 - 11.0	Moderate	5		22.5		
	11.1 - 16.7	Low	2		9.0		
	16.8 - 26	Very low	1		4.5		
Sum						208	100

2.1.5 Dune Survey

The dune survey was conducted in two phases. A first phase took place to identify the most common vegetation present in the dunes utilizing an online key for plant identification (Senckenberg, 2014). A given species of plant was noted down when the frequency exceeded five. The second phase consisted of a more intense survey of the amount of vegetation present and the frequency of the previously identified dominant species. This was done through systematic sampling in lines at right angles to the dunes with a 100 m interval. Along each sampling line through the dunes, the frequency of the species was noted. In addition to this, the length of the line was categorized into five categories: bare sand, grassy, small vegetation (<20 cm height), medium vegetation (<1.5 m height), and large vegetation (>1.5 height).

As a means of data triangulation, the orthorectified image produced as explained in section 2.1.2 was used to perform a supervised classification in ArcGIS Pro on the dunes to check whether the findings from the dune survey were realistic. This supervised classification was performed into three classes: bare sand, grassy, and vegetation. The vegetation classes were bundled together as from the UAV imagery the differences between small, medium, and large vegetation were

ambiguous. Training areas for the supervised classification were spread out across the different classes and throughout the dune areas, to ensure a good spread and decrease the chance of colour balance influencing the classification.

A bivariate map was produced showing the variables vegetation presence and slope.

The slope variable was previously calculated as described in section 2.1.4. The slope was reclassified to be fitted in three classes: low, medium, and high, according to the ranges shown in Table 5.

Table 5 - Classification of slope for bivariate visualisation.

Class	Slope range (°)
Low	0.0 – 9.6
Medium	9.6 – 24.1
High	24.1 – 78.9

2.1.6 Mitigation Strategies

The mitigation strategies have been developed by applying theoretical strategies found in literature. In particular, a report by fellow student David Tsofnas (2023) was used. This report was specially prepared to provide an overview for potential mitigation strategies in a broader context, with limited detailed information available about the study area. These (general) mitigation strategies were considered and further researched to determine the suitability to the specific situation found in the project area, and expanded on where necessary.

2.2 Materials

- DJI Mavic Pro 1
- Agisoft MetaShape
- ArcGIS Pro
- Trimble DA2 Catalyst GNSS System
- Measuring stick (2.5 m)
- Smartphone with GPS capabilities and application (E.g., GPS Essentials)

3 Results

3.1 Base results

Prior to the results of each specific research question, the collected UAV imagery (1050 images) was used to generate an orthorectified mosaic image and Digital Terrain Model, with a spatial accuracy of 4.94 cm (X, Y, Z). During the generation, it was found that one of the twelve collected GCPs fell outside the project area, meaning it was excluded. The Agisoft MetaShape processing report is found in Annex VI.

The generated Digital Terrain Model can be found in Annex VII.

3.2 Coastal Vulnerability Index (SRQ1)

The Coastal Vulnerability Index value was found through the application of Equation 1. The found value for each variable is shown in Table 6. Prior to this, several variables were calculated.

Using the DTM, the slope map in percent rise was generated for the coastal area of the research area (Annex VIII). The coastal slope exceeded >0.2% in all but a few raster cells in the ArcGIS Pro environment. As this was the case, the coastal slope was considered to be homogeneous, all falling within the lowest CVI class (1).

The shoreline erosion rate between 2010 and 2022 was found to be, on average, 2.1 m per year. A selection of the dataset was made as not all Near values were calculated at right angles. Some 500 m of shoreline was found to have accreted at a rate of 1.43 m per year, though this concerns a part of the shoreline just outside the research area boundaries. The data further suggests that the entire shoreline saw an average of 11 m of accretion between 2014 and 2016, the only time jump where the shoreline as a whole saw accretion instead of erosion.

The mean tide range and mean wave height were both found to be 0.8 m.

Table 6 - Results for each variable of the CVI calculation.

Variable	Result	CVI Class	Value
Geomorphology, <i>a</i>	Sand beach	Very high	5
Coastal slope, <i>b</i> (%)	All cells >0.2%	Very low	1
Relative sea-level rise rate, <i>c</i> (mm/y)	All scenarios >3.16 (Table 4)	Very high	5
Shoreline erosion / accretion rate, <i>d</i> (m/y)	-2.1	Very high	5
Mean tide range, <i>e</i> (m)	0.8 m	Very high	5
Mean wave height, <i>f</i> (m)	0.8 m	Low	2

Using these variables, we calculate the CVI to be, $CVI = \sqrt{\left(\frac{5*1*5*5*5*2}{6}\right)} = 14.43$, classified as very high.

3.3 Terrestrial Flood Hazard (SRQ2)

A visualisation of the terrestrial flood hazard is shown in Figure 3. Notably, the high and very high classes of terrestrial flood hazard make up the majority of the area. There is a limited area classified as low or very low, making up only 3%. Visualisations of the individual factors contributing to the terrestrial flood hazard can be found in Annex VII (DTM), Annex IX (Slope) and Annex X (Flow Accumulation).

Terrestrial flood hazard map of research area

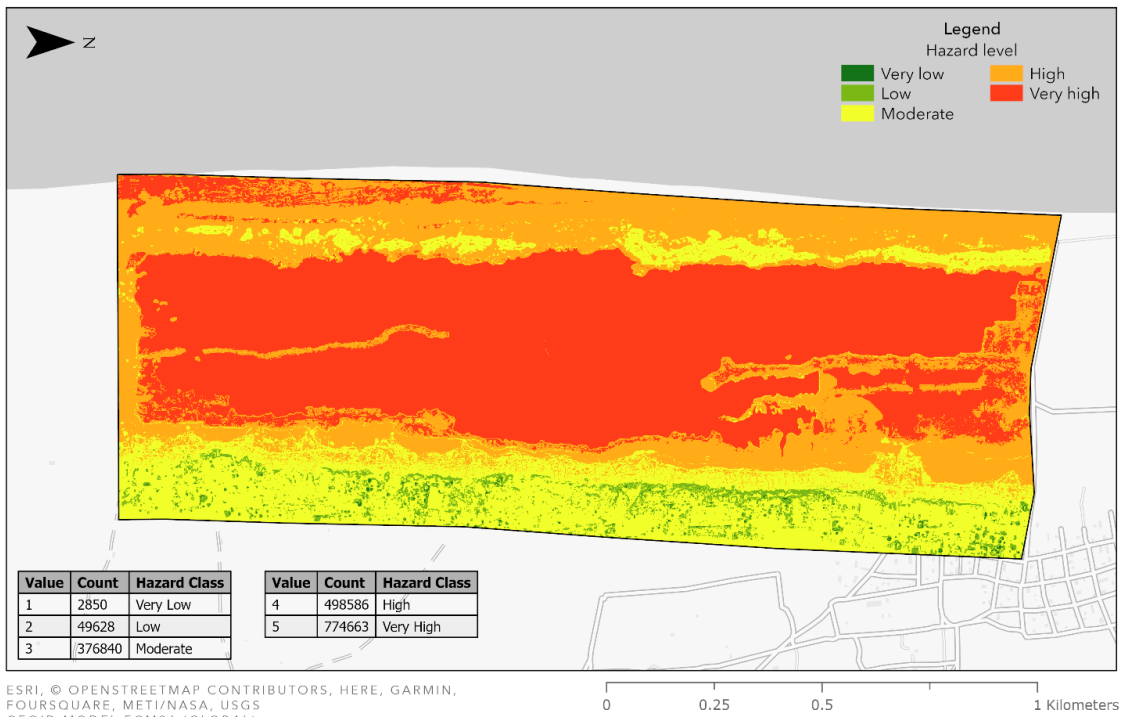


Figure 3 - Visualisation of terrestrial flood hazard.

3.4 Dune Survey (SRQ3)

Results from the field survey, shown in Table 7, show that bare sand and grassy areas make up the majority of the dune areas. From the vegetation, medium vegetation is the most prevalent category.

Table 7 - Results from in-field dune survey.

Distance from Northern edge (m)	% bare sand	% grassy	% small vegetation (<20 cm)	% medium vegetation (<1.5 m)	% large vegetation (>1.5 m)
0	35	45	0	19	0
100	50	27	1	20	0
200	32	32	0	34	1
300	76	6	9	9	0
400	45	36	9	9	0
500	28	22	28	23	0
600	25	31	6	38	0
700	37	26	2	6	30
800	33	47	5	13	2
900	32	46	0	12	10
1000	29	49	8	12	2
1100	22	66	8	4	0
1200	19	67	2	10	2
1300	27	56	4	13	0
1400	37	48	8	5	0
1500	32	39	1	23	4
1600	38	47	3	12	0
1700	41	34	9	9	8
1800	49	43	1	7	0
1900	53	27	0	16	4
2000	67	24	2	7	0
Average	38.4	39.0	5.0	14.3	3.0

The supervised raster classification, the result of which can be seen in Figure 4 (next page), show a comparable division between sandy, grassy, and vegetated dune areas, as summarized in Table 8.

Table 8 - Results of supervised classification of dune areas.

Class	Pixel Count	Percentage of Total
Sand	147178	41.6
Grass	139899	39.5
Vegetation	66778	18.9

The slope (°) map, based on the DTM of the study area (Annex VII), for the dunes can be seen in Figure 5 on the next page.

Dune vegetation classification

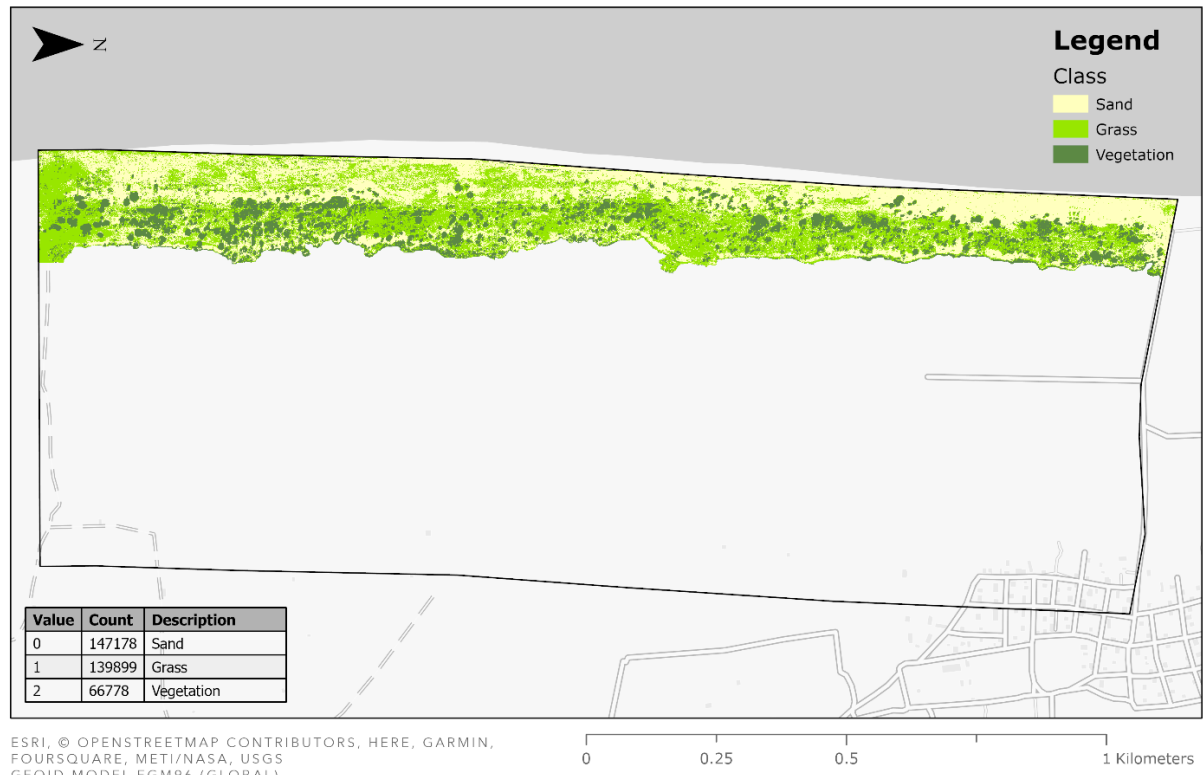


Figure 4 - Visualisation of dune vegetation classification.

Dune slope classification

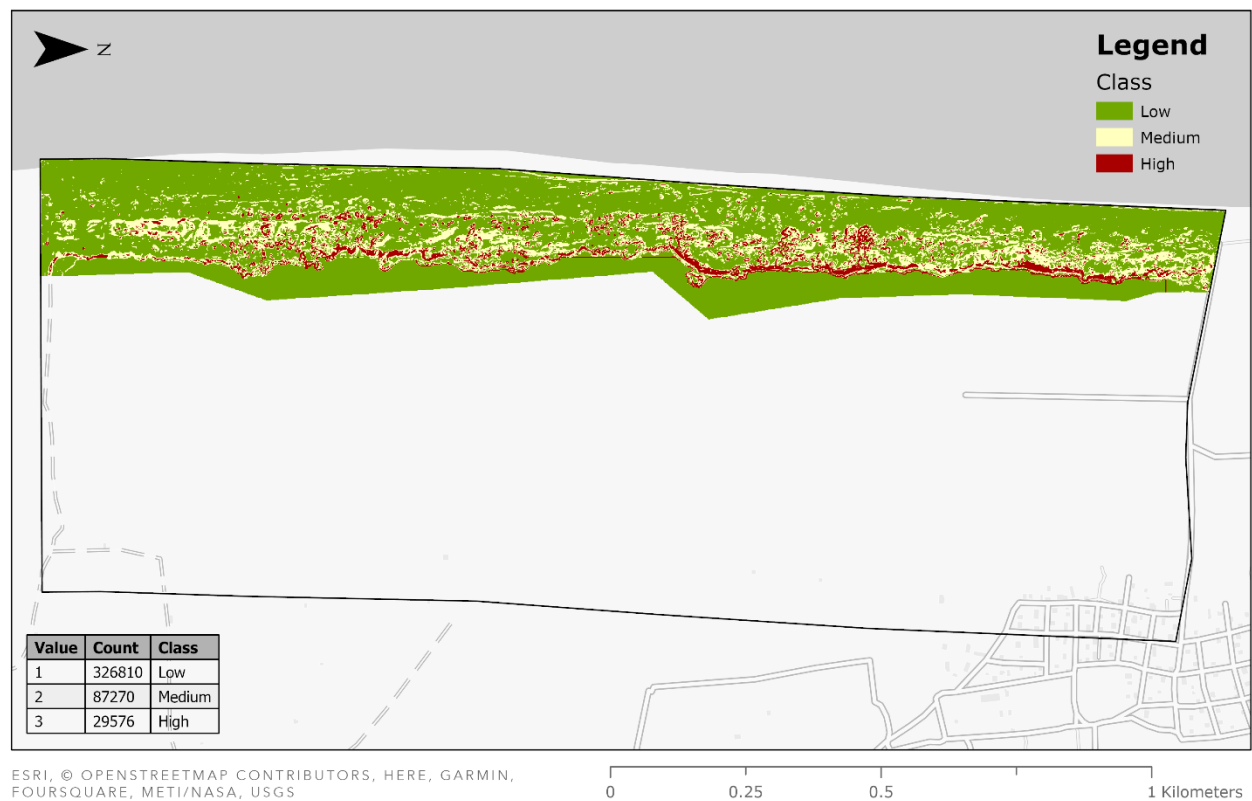


Figure 5 - Visualisation of dune slope classification.

The bivariate visualisation of the relationship between the vegetation presence and slope can be seen in Figure 6. Areas of note are the steep dune edges towards the lake side of the project area, which are largely unvegetated.

During the dune survey, a relative abundance of the species *Gymnosporia senegalensis* was found, as shown in Table 9.

Table 9 - Results of species identification and frequency during dune survey.

Species	Frequency
Acacia hebeclada DC.	13
Cleistanthus ripicola J. Léonard	12
<i>Gymnosporia senegalensis</i>	33
Neocarya macrophylla (Sabine) Prance	9

Bivariate map of slope and vegetation class

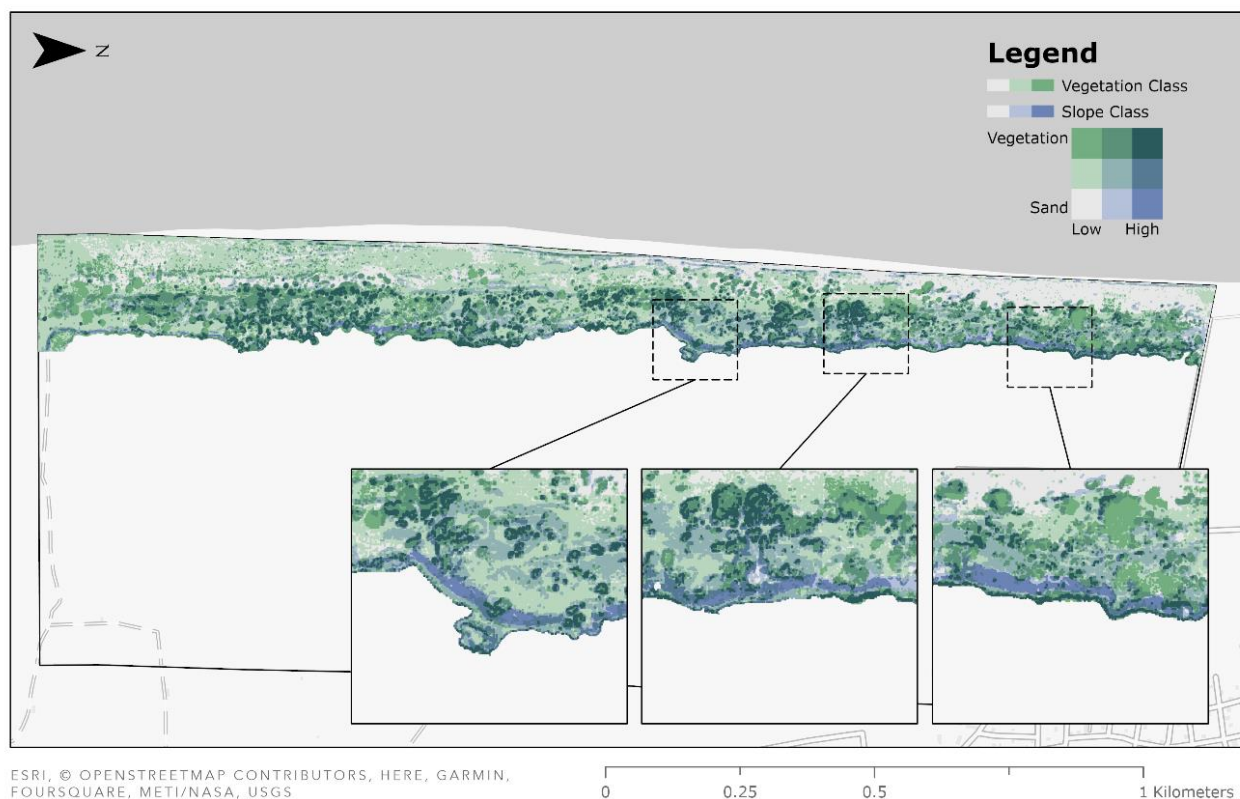


Figure 6 - Bivariate visualisation of dune survey results.

3.5 Mitigation Strategies (SRQ4)

From the preliminary research conducted by David Tsofnas (2023), several key intervention methods were identified that are suitable for the context of the research area and researched further. An overview of the potential benefits of the identified mitigation strategies is found in Table 10 below, with more detailed explanations in the following sections. At the end of this chapter, Figure 7 visualises the appropriate locations for the possible mitigation strategies.

Table 10 - Overview of possible mitigation strategies.

Strategy	Aimed at	Benefits	Potential for study area
Cobble beaches	Reducing coastal vulnerability	Lower geomorphology vulnerability class, reduced coastal erosion	Limited
Soft nourishment of the coast	Reducing coastal vulnerability	Wider beach, natural dune growth stimulation	Moderate
Groynes	Reducing coastal vulnerability	Reducing erosion / increasing accretion	Great
(Vegetated) semi-circular bunds	Precipitation interception	Decreases slope, increases infiltration, increases interception	Moderate
Gully structures	Reduce gully flow, prevent gully expansion, reduce erosion	Reduces flow velocity, increases infiltration	Limited
Bottom withdrawal spillway	Precipitation discharge	Stabilise water level in the lake	Great
Increasing vegetation	Improve dune stability	Decreased wind erosion, decreased surface erosion, higher stability	Great
Sand-trapping fences	Increase dune volume	Capture wind-blown sand, aid in formation of foredunes	Moderate

3.5.1 Strategies aimed at reducing coastal vulnerability

From the findings of the CVI, several approaches can be taken to reduce the coastal vulnerability, corresponding to two factors which are ranked as 'very high' and which can be considered for short-term mitigation. The reduction of the relative sea-level rise falls outside the scope of this study, and it is generally accepted that the tide range is determined by gravitational processes that are difficult, if not impossible, to be influenced by humans. Factors where intervention is possible are the changing of the geomorphology and the reduction of shoreline erosion, factors which are somewhat related.

The changing of the geomorphology of the coastline is a challenging project, though technically possible. For example, the changing of the geomorphology to a cobble beach through the

introduction of pebbles and cobbles would change the variable class from very high to high. Furthermore, the introduction of pebbles or rocks is also used as a measure of reducing the coastal erosion rate, meaning two CVI variables are changed through one strategy (Bayle et al., 2020). However, considering the scale of this undertaking, it may not be a realistic or ideal strategy. It would also change the environment substantially, which may not be desired considering the tourism applications of the study area. As this strategy is demanding on the environment with high input, with limited benefits, the potential is also limited.

Other approaches, aimed at reducing the coastal erosion are likely more suitable in this case. A range of approaches is available with varying potential benefits, as summarised by Van Rijn (2011), varying between erosion control through soft nourishments and hard structures, with Rangel-Buitrago et al. (2018) stating that "... the protection approach using hard structures is widely perceived as the best coastal erosion management practice".

Research shows that soft nourishment leads to a higher erosion rate at the main site of deposition, but accretion in the surrounding areas, with as added benefit that it stimulates natural dune formation, which may aid in improving the dune structure in the study area (Huisman et al., 2021). Furthermore, the added beach width will allow the erosion processes to be weathered for a longer time. A major drawback is the expense, both in resources and labour, for applying soft nourishment, and the temporary nature of the strategy.

Hard structures, such as groynes, are often cheaper and easier to implement, whilst still bringing considerable benefits. A case study from India shows that the construction of groynes can increase the accretion rate by up to 5.15 m/y (Pradeep et al., 2022). Similar results in the study area would reduce the shoreline erosion factor of the CVI to class low or very low, and could decrease the overall CVI to 9.13 or 6.45 respectively. Furthermore, they are likely less disruptive to the environment and tourists.

3.5.2 Strategies aimed at reducing terrestrial flood hazard

The reduction of the terrestrial flood hazard is a difficult challenge, and realistically it cannot be reduced to the point where there is low or very low hazard throughout the study area, evident by the seasonal lake present. However, a combination of interception methods and discharge structures should allow for the stabilising of the water level in the lake, making it more suitable for project development when compared against the current seasonal water level variance of 1 – 1.5 m.

Interception and infiltration of precipitation can be stimulated in various ways. Logic dictates that these strategies should be located along the eastern edge of the study area, where the largest catchment area is contributing to hydrological flows. The introduction of (leafy) vegetation typically improves the interception. While some areas of the study area already have vegetation present, it could be improved in certain areas. This process may be stimulated to develop in a semi-natural way through the introduction of semi-circular bunds. These bunds have found to be effective at increasing infiltration and promoting vegetative growth through the improvement of soil characteristics (Heshmati et al., 2018; Mousavi et al., 2019). Research by El-Atta (2013) shows a potential runoff reduction of 55% utilising semi-circular bunds. As added benefit, the bunds may reduce the landscape slope over time, promoting higher infiltration rates. Considering the ease of implementation and the benefits of this method, the potential is great. However, it would transform the physical environment substantially, which may not be an attractive prospect to project developers, reducing the potential somewhat.

Through the design and introduction of control structures in the gullies flowing towards the lake, the peak discharge may be reduced and further infiltration stimulated. As gullies are highly variable in size and dynamics, a claim regarding the effectiveness cannot be made based on literature review, and effectiveness is highly dependant on the design, not covered in this study. Despite their relatively expensive construction and management cost, the implementation of gully control structures might be considered, as they have some potential for reducing the discharge into the lake.

The previously described strategies, aimed at increasing interception, infiltration and decreasing peak discharge, may be combined with discharge structures discharging lake water into the sea such as a bottom withdrawal spillway. The combination of these methods should allow for the management of the terrestrial flood hazard, though constant management and monitoring of the lake water level may be required. Detailed designs may be developed based on precipitation data ahead of project development.

3.5.3 Strategies aimed at improving dune structure

As mentioned in section 3.5.1., the dune structure may be improved through the implementation of soft coastal nourishment strategies, though other options are available that are better tailored to the improvement of dune structure. The improvement of the dune structure can be divided into two main categories: improving stability and increasing dune volume.

Introducing (more) vegetation to the dune system can improve the stability of the dune system (Miller, 2015; Tsoar, 2005). Research has highlighted certain species such as *Spinifex littoreus* and *Vitex rotundifolia* to be especially suited for this strategy (Lee et al., 2020), though these species are not native to the Gambia. Furthermore, research shows that in general, underground biomass (root systems) contribute to dune stability (Bryant et al., 2019), and it is generally accepted that the presence of vegetation decreases the amount of surface erosion. The introduction of more (varied) vegetation may also stimulate natural dune formation, thus increasing dune volume (Durán & Moore, 2013). While a relatively cheap and easily implemented strategy, increasing vegetation sees multiple benefits and great potential. Areas where this strategy may be applied to maximise dune stability can be derived from the bivariate dune visualisation presented in Figure 6. To stimulate dune volume increase, vegetation should be introduced in the foredunes.

Another strategy to increase dune volume is the implementation of sand-trapping fences. Research by Eichmanns et al. (2021) summarizes the different combinations of orientation to the shoreline and design type, though concludes there is no 'best' method. However, they go on to state that "some national authorities have published local guidelines for the use of sand trapping fences as a nature-based solution", though the Gambian government has not published any guidelines. Eichmanns et al. (2021) further explore the empirical methods that may be used to determine in detail the effect that a specific sand-trapping fence may achieve, though this falls outside the scope of this research. Research has shown the potential of this strategy for the creation of foredunes and capturing wind-blown sand (Liu et al., 2023). This strategy would be appropriate to implement in areas where foredunes are lacking. Due to the relatively low cost and extensive literature on the implementation methodology, this method shows great potential. However, the fences may be considered (visually) hindering to tourists, so project developers may opt to minimise their use.

Overview of suitable locations for intervention strategies



Figure 7 - Visualisation of suitable locations for discussed intervention strategies.

4 Discussion

4.1 Discussion of Results and Methodology

4.1.1 Coastal Vulnerability Index

Typically, the Coastal Vulnerability Index is used as a comparative scale on a quantile basis, meaning the classification from low to very high is determined based on the CVI values found along the broader shoreline. Due to the scope of this research, only one CVI value was found, so this quantile approach cannot be taken. Even so, an estimation can be made as to what a CVI of 14.43 means. When compared against the USGS study of the U.S. pacific coast from which the methodology was derived, the CVI would be classified as 'very high vulnerability' (USGS, n.d.), though this does not directly mean we can accept this as the vulnerability class, as the U.S. Pacific coastline is not representative of the Gambian coastline. Compared against other literature, the CVI value of 14.43 would be classified as 'high vulnerability' in India (Dwarakish et al., 2009), 'very high vulnerability' in Ghana (Addo, 2013), and 'very high vulnerability' in Greece (Tragaki et al., 2018). No literature was found specifically for the Gambia or West-African coast, with the closest found CVI study conduction in Ghana. Due to the great variability in coastal dynamics depending on location, it is difficult to apply CVI rankings found in other parts in the world to the value found in this study. However, considering that 14.43 is found to be 'high vulnerability' or 'very high vulnerability' in the consulted studies, and considering that four out of six CVI factors are classified as 'very high vulnerability', it is not unreasonable to deduce that the shoreline in the research area is very highly, or at least highly, vulnerable to coastal flooding.

The relatively high shoreline erosion rate of 2.1 m/y calculated for the determination of the CVI, is in line with a previously found erosion rate for the Gambian coast (Gomez et al., 2020). Other studies for the Gambia were not found, but a study in neighbouring country Senegal shows erosion rates of up to 4.39 m/y occurring (Ndour et al., 2018). Other studies have found erosion rates of up to 9 m/y in Algeria (Sallaye et al., 2022). However, erosion and accretion processes are highly dependant on the local geomorphology and wave dynamics of a shoreline, so care should be taken when comparing. Even so, it is a worryingly high rate of erosion, that could lead to the complete erosion of the beach in 40-50 years, assuming the erosion rate stays the same, though research suggests this will increase with rising sea levels (Zhang et al., 2004). Looking at the data, an interesting observation can be made when looking at the erosion rate between 2014 and 2016, where we see a sudden jump of some 20 metres. It is likely this jump is due to the change in resolution between the Landsat 8 and Sentinel 2 imagery used for the respective years, as the spatial resolution increases from 30 m to 10 m, as no other reasons for a sudden increase in erosion rate for this timeframe can be found.

To improve the methodology, the CVI may be adapted, as has been done in other studies in different regions (Gerrity et al., 2018; Martínez-Graña et al., 2018; Pantusa et al., 2022), to include specific variables that may be especially relevant in the Gambian or West-African context. One may also divide the coastline into 'blocks' and calculate the CVI, so that the comparative nature of the methodology may be benefitted from. Further improvements can be achieved through more robust data collection regarding tide range and wave height, compared against the predictive values used in this study. Furthermore, attention might be paid to the classification of relative sea-level rise, as the classification developed in 1998 may no longer be particularly relevant to the climatological conditions today. Finally, the method of shoreline digitization to determine the rate of coastal erosion can be improved by making it automatic, rather than manual, removing the subjectivity and potential human error. The application of automatic shoreline digitization may lead to lower error and also allows the consideration of tidal height (Dewi, 2019; Dewi & Bijker, 2020; Vos et al., 2019).

4.1.2 Terrestrial Flood Hazard

The visualisation of the terrestrial flood hazard as shown in Figure 3 - Visualisation of terrestrial flood hazard. Figure 3 displays a worrying image, with the majority of the study area being classified as high or very highly vulnerable to terrestrial flooding. In particular, the middle section of the study is dominantly classified as very highly vulnerable, which is logical considering the area is seasonally flooded due to precipitation from the monsoon period. Areas surrounding the

lake are found to be at high hazard level, suggesting that with changing climatic conditions or precipitation patterns, such as a particularly extreme precipitation event or longer monsoon period, the areas may flood. Similar to the CVI, the hazard is expressed as a comparative scale, something to be mindful of when comparing against literature. Furthermore, due to the unique combination of data collection and processing methodology, it is difficult to compare the results found against literature as literature generally is based on applying the methodology on satellite imagery, instead of UAV imagery. Even so, the application of the multi-criteria methodology used in this study has also been applied in varying forms to case studies throughout the world (Melesse et al., 2015; Raaijmakers et al., 2008). Though not much can be commented on the results due to the differences in landscape, the methodologies applied are similar and even applied for mitigation strategy development, lending credence to the method used in this study.

The Flow Accumulation factor map (Annex X) highlights the fact that the study area drains towards the lake in the middle. Furthermore, some clear accumulation patterns are visible along the eastern slope of the study area, where water from the higher lying inland will stream towards the lake. Intervention measures aimed at increasing interception and infiltration, like the semi-circular dunes suggested in section 3.5.2., will likely be effective if implemented in these areas.

Improvement of the methodology may be achieved through the application of different flow algorithms. Due to the computational demand, the D8 algorithm is used, though the D ∞ or MFD algorithm will likely produce more realistic results (Ma & Wang, 2022). Furthermore, the generation of the DTM might be done with a more aggressive depth filtering. Even though care was taken to remove most non-surface objects, some remain as seen in Annex VII. Finally, it may be worthwhile to exclude the lake area from the flow accumulation map. This would provide a clearer picture of where areas are that might flood in the future, rather than the areas that are already flooded. Furthermore, it would allow a better analysis of where mitigation structures could be placed.

4.1.3 Dune Survey

Through the bivariate visualisation (Figure 5), in particular the highlighted sections, the results of the dune survey should be interpreted as worrying. There are areas of the dune system completely bare and at steep angles (>24 degrees). Depending on the texture, moisture and drying time, the angle of internal friction of sand is found between 37 and 48 degrees (Avci & Mollamahmutoğlu, 2018). Without the presence of vegetation contributing to stability and below-ground biomass, it is likely that these steeply sloped areas are at risk of failure and high rates of erosion (Bryant et al., 2019; Renard, 1991). High erosion rates may cause the dunes to fail quicker, which in turn might have disastrous effects on the study area – as it opens up the possibility of coastal floodings spilling over into the lower lying areas of the study area. The process of dune failing is unlikely to be a fast-paced process and may take decades to occur. Even so, considering the proposed application of the area, it may not be considered sustainable (tourism) investment to develop a location that may suffer dune failures in the coming decades.

The methodological quality of this part of the study may be improved through more accurate materials during the cross-sectional surveys of the dunes or through visiting the study area in another season so that the vegetation can be identified whilst flowering and alive, compared to being dried out as found during this study.

4.2 Validity and Reliability

4.2.1 Validity

In general, the internal validity of this study is considered to be medium to high by the researcher. Appropriate materials and methodology have been applied in the pursuit of valid results, though at times time constraints have resulted in less-than-ideal materials or methods, with a negative effect on the validity, with potential means of improvement described per result in the previous subchapter.

The broader implications of this study should also be considered, as the situation found in the TDA near Gunjur is not unique to Gunjur. In fact – large sections of the Gambian coastline were observed to be in very similar, if not worse states, during the field work in the Gambia. Stretches of the coast to the North of the study area were observed to have far lower and thinner dunes and beachfronts. As almost the entire Gambian coast is assigned as TDA, and large sections of the coastline have seen similar patterns of sand excavation, the findings of this study may be taken to be fairly representative of the issues facing the Gambian coast. Furthermore, the CVI classification of ‘very high vulnerability’ is likely applicable to the majority of the Gambian coast, as the coastline is fairly homogenous to the situation found in the study area. This study also provides an overview of potential mitigation that may be considered when facing similar issues, regardless of the location. The preference for certain strategies may differ in different situations, but the strategies proposed are likely to have a positive effect in one way or another – and the strategies should therefore be carefully considered on a case by case basis.

This study further shows that UAV imagery – even from widely available commercial UAVs - is suitable to be applied for small scale flood hazard mapping. More powerful hardware would also allow for greater areas to be covered. At the same time, the increased resolution poses some new challenges in the form of computational demands and the representation of small divots with regards to flow algorithms in the ArcGIS Pro environment.

4.2.2 Reliability

This study is unlikely to have a high reliability. The data collection methods and data acquired are considered to be reliable, though several methods applied after the data collection phase were subjective, reducing the reliability.

Regarding data collection, there is some unreliability in the UAV imagery / GCP collection. The GCPs were collected with a horizontal and vertical accuracy of 1 cm, making them very reliable. However, during the georeferencing of the UAV imagery this accuracy decreased to some 5 cm, as can be seen in the Agisoft MetaShape processing report excerpt in Annex VI. If this study was repeated, some minor discrepancies may be found due to this level of accuracy.

During data collection, the most unreliable phase was the collection of underwater datapoints. During data collection on open water with the boat, points were collected on an ad hoc basis, making it difficult to repeat the exact measurements. Furthermore, although the same Trimble system was used, the accuracy during this stage of data collection was lower, at some 30 cm. Less reliable was the measurements around the lake edge utilizing the measuring stick. At this point, the Trimble system was no longer available for use, and instead a mobile phone application was used, reducing the GPS point collection accuracy to some 4 m. This resulted in some points being incorrectly shown to have been collected on land, rather than in the water, an issue later resolved by hand in the ArcGIS environment through moving the datapoints into the water area, reducing the reliability.

The creation of the DTM was reliable, up until the manual filtering phase. The manual removing of some areas is a subjective process, and thus cannot be repeated exactly, reducing reliability. The combination of the DTM with the IDW is reliable, as this can be repeated exactly in the ArcGIS environment.

Though the calculation of the CVI itself is reliable, based on the variables found and calculated, the determination of the shoreline erosion rate is not reliable. The shoreline digitization was largely done by hand rather than using a model or algorithm, making it very susceptible to

subjectivity and human error. Arguably, this is the largest source of unreliability in this study, and improving the methodology for this section would improve the overall reliability.

The determination of the terrestrial flood hazard class was done through a reliable method that can be repeated easily through following the described workflow in section 2.1.4.

Finally, the dune survey is fairly reliable. The methodology applied can be repeated, though there is a level of inaccuracy due to the use of a smartphone-based application to determine where each cross-section of the dune should be walked. This application has an accuracy of 4 m, and so repeats may yield differing results.

5 Conclusion

5.1 General Conclusion

Reflecting on the general and specific research questions stated at the beginning of this thesis, several conclusions are drawn. Firstly, through this study it has been shown that the shoreline in the proposed Tourism Development Area near Gunjur, Gambia, is highly vulnerable to coastal flooding, determined through the calculation of the Coastal Vulnerability Index. Secondly, the majority of the study area is classified as high or very high hazard for terrestrial flooding, especially the low-lying centre of the site that was previously used as sand excavation grounds – further evident by its seasonal flooding. It may not be realistic to aim to remove this hazard, so options of project development with a lake present may be beneficial. Furthermore, the dunes within the study area have been found to be at risk of erosive processes and potentially failing in the future due to steep slopes and lack of vegetation.

Considering the context of the research area, having been assigned as a potential location for tourism destination development, project developers and investors should be mindful of the presented findings and recommendations. Investing in the area without consideration of the hazards and vulnerability of the area may lead to disaster in the future, and likely a (financially) unsustainable venture. Therefore, plans for developing this area should include mitigation strategies for the issues found.

This study can also serve as an exploration of issues that the broader Gambian coast may face in the future. The situation found in the study area is not unique and is seen in many places along the coastline. Considering the results found in this study, the current coastal management practices in place in the Gambia might have to be reconsidered, as they leave sections of the coast vulnerable to coastal flooding, terrestrial flooding, and dune failure.

5.2 Recommendations

As mentioned before in this study, there is room for the implementation of mitigation strategies in the study area that can likely prevent or influence processes in such a way as to minimize the coastal flooding vulnerability and terrestrial flood hazard. Examples of these strategies have previously been given, but it is difficult to determine which of these mitigation strategies should take priority. Both coastal flooding and terrestrial flooding pose a realistic threat, and thus the mitigation strategy that takes priority is dependant on the wishes of a potential project developer.

Prior to any choices regarding the implementation of mitigation strategies, the knowledge acquired in this study can be expanded upon and researched more thoroughly. The relatively broad approach taken in this study may not reflect all small-scale, intricate systems at play to a degree whereat mitigation strategies can be designed to be at their most effective. However, based on the findings of this study, the researcher recommends the following combination of mitigation strategies in the research area:

Construction of groynes, to reduce the rate of coastal erosion, reducing the coastal vulnerability to flooding.

Increasing vegetation on steep, bare slopes in the dunes and placement of sand-trapping fences in front of the foredunes, stimulating dune growth and stability as natural defence mechanism against coastal flooding.

Vegetated semi-circular earth bunds in barren areas in the East of the study area, preferably in areas where flow accumulation is found, to reduce the runoff to lower-lying areas through interception and infiltration of precipitation.

Design and implementation of one or several bottom withdrawal spillways from the lake to the sea, to create the discharge capacity required to stabilise the lake water level during (extreme) precipitation events, such as during the monsoon.

The exact effectiveness of these strategies may be explored further during a potential design phase using empirical methodology or modelling.

To gain insight into how these issues of coastal flooding vulnerability and terrestrial flooding hazard present in a broader context, a larger-scale study might be relevant. The determination of the Coastal Vulnerability Index for the Gambian, or West-African coast as a whole, would be a worthwhile exercise that can contribute to future-proof coastal management.

References

- Addo, K. A. (2013). Assessing Coastal Vulnerability Index to Climate Change: the Case of Accra – Ghana. *Journal of Coastal Research*, 165, 1892–1897. <https://doi.org/10.2112/si65-320.1>
- Annis, A., Nardi, F., Petroselli, A., Apollonio, C., Arcangeletti, E., Tauro, F., Belli, C., Bianconi, R., & Grimaldi, S. (2020). UAV-DEMs for Small-Scale Flood Hazard Mapping. *Water*, 12(6), 1717. <https://doi.org/10.3390/w12061717>
- Avci, E., & Mollamahmutoğlu, M. (2018). Syneresis dependent shear strength parameters of sodium silicate grouted sands. *Quarterly Journal of Engineering Geology and Hydrogeology*, 52(1), 99–109. <https://doi.org/10.1144/qjegh2017-080>
- Ayeni, R. K. (2020). Determinants of private sector investment in a less developed country: a case of the Gambia. *Cogent Economics & Finance*, 8(1), 1794279. <https://doi.org/10.1080/23322039.2020.1794279>
- Bayle, P. M., Blenkinsopp, C., Conley, D. J., Masselink, G., Beuzen, T., & Almar, R. (2020). Performance of a dynamic cobble berm revetment for coastal protection, under increasing water level. *Coastal Engineering*, 159, 103712. <https://doi.org/10.1016/j.coastaleng.2020.103712>
- Blumenfeld, J. (2021). Data Processing Levels. *Earthdata*. <https://www.earthdata.nasa.gov/engage/open-data-services-and-software/data-information-policy/data-levels>
- Bosch, T., Colijn, F., Ebinghaus, R., Kötzinger, A., Latif, M., Matthiessen, B., Melzner, F., Oschlies, A., Petersen, S., Proelß, A., Quaas, M., Requate, T., Reusch, T., Rosentiel, P., Schrottke, K., Siebert, U., & Soltwedel, R. (2010). *World Ocean Review: Chapter 3: The uncertain future of the coasts*. maribus. Retrieved June 14, 2023, from https://worldoceanreview.com/wp-content/downloads/wor1/WOR1_en.pdf
- Bryant, D. B., Hoch, C., Provost, L. A., Bell, G. F., & Bryant, M. A. (2019). *THE ROLE OF BELOWGROUND BIOMASS ON SHORT TERM DUNE EVOLUTION*. https://doi.org/10.1142/9789811204487_0105
- Consequences of climate change*. (n.d.). Climate Action. Retrieved June 14, 2023, from https://climate.ec.europa.eu/climate-change/consequences-climate-change_en
- Development and importance of tourism for Gambia*. (n.d.). Worlddata.info. Retrieved December 12, 2022, from <https://www.worlddata.info/africa/gambia/tourism.php>
- Dewi, R. (2019). Monitoring long-term shoreline changes along the coast of Semarang. *IOP Conference Series*, 284(1), 012035. <https://doi.org/10.1088/1755-1315/284/1/012035>
- Dewi, R., & Bijker, W. (2020). Dynamics of shoreline changes in the coastal region of Sayung, Indonesia. *The Egyptian Journal of Remote Sensing and Space Science*, 23(2), 181–193. <https://doi.org/10.1016/j.ejrs.2019.09.001>
- Diaconu, D. C., Bui, D. T., & Popa, M. (2021). An Overview of Flood Risk Analysis Methods. *Water*, 13(4), 474. <https://doi.org/10.3390/w13040474>
- Durán, O., & Moore, L. J. (2013). Vegetation controls on the maximum size of coastal dunes. *Proceedings of the National Academy of Sciences of the United States of America*, 110(43), 17217–17222. <https://doi.org/10.1073/pnas.1307580110>

- Dwarakish, G., Vinay, S., Natesan, U., Asano, T., Kakinuma, T., Venkataramana, K., Pai, B. J., & Babita, M. (2009). Coastal vulnerability assessment of the future sea level rise in Udupi coastal zone of Karnataka state, west coast of India. *Ocean & Coastal Management*, 52(9), 467–478. <https://doi.org/10.1016/j.ocemoaman.2009.07.007>
- Eichmanns, C., Lechthaler, S., Zander, W., Pérez, M., Blum, H., Thorenz, F., & Schüttrumpf, H. (2021). Sand Trapping Fences as a Nature-Based Solution for Coastal Protection: An International Review with a Focus on Installations in Germany. *Environments*, 8(12), 135. <https://doi.org/10.3390/environments8120135>
- El-Atta, H. A. (2013). Comparative efficiency of rainwater harvesting by some types of microcatchments. <https://www.cabdirect.org/cabdirect/abstract/20133417181>
- European Space Agency [ESA]. (n.d.). *Copernicus Open Access Hub* [Dataset]. <https://scihub.copernicus.eu/dhus/#/home>
- Gerrity, B. F., Phillips, M., & Chambers, C. (2018). Applying a Coastal Vulnerability Index to San Mateo County: Implications for Shoreline Management. *Journal of Coastal Research*, 85, 1406–1410. <https://doi.org/10.2112/si85-282.1>
- Gomez, M. L. A., Adelegan, O. J., Ntajal, J., & Trawally, D. (2020). Vulnerability to coastal erosion in The Gambia: Empirical experience from Gunjur. *International Journal of Disaster Risk Reduction*, 45, 101439. <https://doi.org/10.1016/j.ijdrr.2019.101439>
- Herring, S. C., Christidis, N., Hoell, A., & Stott, P. A. (2022). Explaining Extreme Events of 2020 from a Climate Perspective. *Bulletin of the American Meteorological Society*, 103(3), S1–S129. <https://doi.org/10.1175/bams-explainingextremeevents2020.1>
- Heshmati, M., Gheitury, M., & Hosseini, M. R. (2018). Effects of runoff harvesting through semi-circular bund on some soil characteristics. *Global Journal of Environmental Science and Management*, 4(2), 207–216. <https://doi.org/10.22034/gjesm.2018.04.02.008>
- Hirabayashi, Y., Tanoue, M., Sasaki, O., Zhou, X., & Yamazaki, D. (2021). Global exposure to flooding from the new CMIP6 climate model projections. *Scientific Reports*, 11(1). <https://doi.org/10.1038/s41598-021-83279-w>
- Huisman, B. J. A., Wijsman, J. W. M., Arens, S. M., Vertegaal, C. T. M., Van Der Valk, L., Van Donk, S. C., Vreugenhil, H. S. I., & Taal, M. D. (2021). *Evaluatie 10 jaar Zandmotor*. Retrieved July 12, 2023, from <https://23g-sharedhosting-zandmotor.s3.eu-west-1.amazonaws.com/app/uploads/2021/06/21114926/Evaluatie-van-10-jaar-Zandmotor.pdf>
- Iizuka, K., Itoh, M., Shiodera, S., Matsubara, T., Dohar, M., & Watanabe, K. (2018). Advantages of unmanned aerial vehicle (UAV) photogrammetry for landscape analysis compared with satellite data: A case study of postmining sites in Indonesia. *Cogent Geoscience*, 4(1), 1498180. <https://doi.org/10.1080/23312041.2018.1498180>
- IPCC. (2021). *Climate Change 2021: The Physical Science Basis. Contribution of Working Group I to the Sixth Assessment Report of the Intergovernmental Panel on Climate Change*. Cambridge University Press. Retrieved June 14, 2023, from <https://www.ipcc.ch/report/ar6/wg1/>
- IPCC. (2023). *Climate Change 2023 Synthesis Report, Summary for Policymakers: A Report of the Intergovernmental Panel on Climate Change. Contribution of Working Groups I, II and III to the Sixth Assessment Report of the Intergovernmental Panel on Climate Change*. Retrieved June 14, 2023, from https://www.ipcc.ch/report/ar6/syr/downloads/report/IPCC_AR6_SYR_SPM.pdf

- Jadama, A. (2021, August 4). Gov't urged to stop illegal sand mining in Gunjur. *The Gambia | Standard News From the Gambia*. Retrieved January 17, 2023, from <https://standard.gm/govt-urged-to-stop-illegal-sand-mining-in-gunjur0/>
- Kourgialas, N. N., & Karatzas, G. P. (2011). Flood management and a GIS modelling method to assess flood-hazard areas—a case study. *Hydrological Sciences Journal-journal Des Sciences Hydrologiques*, 56(2), 212–225.
<https://doi.org/10.1080/02626667.2011.555836>
- Lee, J., Yen, L., Chu, M., Lin, Y., Chang, C., Lin, R., Chao, K., & Lee, M. (2020). Growth Characteristics and Anti-Wind Erosion Ability of Three Tropical Foredune Pioneer Species for Sand Dune Stabilization. *Sustainability*, 12(8), 3353.
<https://doi.org/10.3390/su12083353>
- Liu, J., Wu, J., & Kimura, R. (2023). Evaluating the Sand-Trapping Efficiency of Sand Fences Using a Combination of Wind-Blown Sand Measurements and UAV Photogrammetry at Tottori Sand Dunes, Japan. *Remote Sensing*, 15(4), 1098.
<https://doi.org/10.3390/rs15041098>
- Ma, X., & Wang, A. (2022). Do Model Results Vary under Different Routing Algorithms Based on a Distributed Ecohydrological Model? *Journal of Hydrometeorology*, 23(12), 1913–1928. <https://doi.org/10.1175/jhm-d-21-0251.1>
- Malczewski, J. (2000). On the Use of Weighted Linear Combination Method in GIS: Common and Best Practice Approaches. *Transactions in Gis*, 4(1), 5–22.
<https://doi.org/10.1111/1467-9671.00035>
- Martínez-Graña, A. M., Gómez, D. H. A., Santos-Francés, F., Bardají, T., Goy, J. L., & Zazo, C. (2018). Analysis of Flood Risk Due to Sea Level Rise in the Menor Sea (Murcia, Spain). *Sustainability*, 10(3), 780. <https://doi.org/10.3390/su10030780>
- Melesse, A. M., Zeinivand, H., & Besharat, M. (2015). Flood hazard zoning in Yasooj region, Iran, using GIS and multi-criteria decision analysis. *Geomatics, Natural Hazards and Risk*, 7(3), 1000–1017. <https://doi.org/10.1080/19475705.2015.1045043>
- Miller, T. F. (2015). Effects of disturbance on vegetation by sand accretion and erosion across coastal dune habitats on a barrier island. *Aob Plants*, 7.
<https://doi.org/10.1093/aobpla/plv003>
- Mining and Quarrying - MoPE, The Gambia*. (n.d.). Retrieved January 16, 2023, from <https://www.mope.gm/mining-and-quarrying>
- Mousavi, S. M., Masoudi, M., & Gholami, P. (2019). Effects of Semi- Circular Bunds on Composition, Biodiversity and Biomass changes of Vegetation in Semi-arid Rangelands of Bushehr Province. *Desert Ecosystem Engineering Journal*, 2(2), 23–30.
<https://doi.org/10.22052/jdee.2020.173255.1048>
- Najibi, N., & Devineni, N. (2017). Recent trends in the frequency and duration of global floods. *Earth System Dynamics Discussions*, 9(2), 757–783. <https://doi.org/10.5194/esd-9-757-2018>
- Ndour, A., Laibi, R., Sadio, M., Degbe, C. G. E., Diaw, A. T., Oyédé, L. M., Anthony, E. J., Dussouillez, P., Sambou, H., & Diéye, E. H. B. (2018). Management strategies for coastal erosion problems in west Africa: Analysis, issues, and constraints drawn from the examples of Senegal and Benin. *Ocean & Coastal Management*, 156, 92–106.
<https://doi.org/10.1016/j.ocecoaman.2017.09.001>

- Novelli, M., Gussing Burgess, L., Jones, A., & Ritchie, B. W. (2018). 'No Ebola. . .still doomed' – The Ebola-induced tourism crisis. *Annals of Tourism Research*, 70, 76–87. <https://doi.org/10.1016/j.annals.2018.03.006>
- Pantusa, D., D'Alessandro, F., Frega, F., Francone, A., & Tomasicchio, G. R. (2022). Improvement of a coastal vulnerability index and its application along the Calabria Coastline, Italy. *Scientific Reports*, 12(1). <https://doi.org/10.1038/s41598-022-26374-w>
- Pradeep, J., Shaji, E., S, S. N., Ajas, H., Chandra, S. S. V., Dev, S. D., & Babu, D. S. S. (2022). Assessment of coastal variations due to climate change using remote sensing and machine learning techniques: A case study from west coast of India. *Estuarine, Coastal and Shelf Science*, 275, 107968. <https://doi.org/10.1016/j.ecss.2022.107968>
- Raaijmakers, R., Krywkow, J., & Van Der Veen, A. (2008). Flood risk perceptions and spatial multi-criteria analysis: an exploratory research for hazard mitigation. *Natural Hazards*, 46(3), 307–322. <https://doi.org/10.1007/s11069-007-9189-z>
- Rangel-Buitrago, N., De Jonge, V. N., & Neal, W. A. (2018). How to make Integrated Coastal Erosion Management a reality. *Ocean & Coastal Management*, 156, 290–299. <https://doi.org/10.1016/j.ocecoaman.2018.01.027>
- Renard, K. G. (1991, January 1). *RUSLE: Revised universal soil loss equation*. Journal of Soil and Water Conservation. <https://www.jswconline.org/content/46/1/30>
- Sallaye, M., Mezouar, K., Dahmani, A., & Cherif, Y. S. (2022). Coastal vulnerability assessment and identification of adaptation measures to climate change between Cape Matifou and Cape Djinet, Algeria. *Zenodo (CERN European Organization for Nuclear Research)*. <https://doi.org/10.5281/zenodo.7493268>
- Sand Mining: Gambia's miss-opportunities – Know Your Budget*. (n.d.). Retrieved January 16, 2023, from <https://gambiaparticipate.org/knowyourbudget/investigative-reports/sand-mining-gambias-miss-opportunities/>
- Senckenberg. (2014, March 1). *African Plants - A Photo Guide - Home*. Retrieved June 21, 2023, from http://www.africanplants.senckenberg.de/root/index.php?page_id=81
- The effects of sand mining*. (2022, October 5). The Point. Retrieved January 16, 2023, from <https://thepoint.gm/africa/gambia/editorial/the-effects-of-sand-mining>
- Tide table for Bakau*. (n.d.). Tide Forecast. Retrieved June 19, 2023, from https://www.tide-forecast.com/locations/Bakau/forecasts/latest/six_day
- Tragaki, A., Gallousi, C., & Karymbalis, E. (2018a). Coastal Hazard Vulnerability Assessment Based on Geomorphic, Oceanographic and Demographic Parameters: The Case of the Peloponnese (Southern Greece). *Land*, 7(2), 56. <https://doi.org/10.3390/land7020056>
- Tragaki, A., Gallousi, C., & Karymbalis, E. (2018b). Coastal Hazard Vulnerability Assessment Based on Geomorphic, Oceanographic and Demographic Parameters: The Case of the Peloponnese (Southern Greece). *Land*, 7(2), 56. <https://doi.org/10.3390/land7020056>
- Tsoar, H. (2005). Sand dunes mobility and stability in relation to climate. *Physica D: Nonlinear Phenomena*, 357(1), 50–56. <https://doi.org/10.1016/j.physa.2005.05.067>
- Tsofnas, D. (2023). *Flood prevention and coastline restoration methods for the west African coastline*.

Tyukavina, A., Potapov, P., Hansen, M. C., Pickens, A. H., Stehman, S. V., Turubanova, S., Parker, D. M., Zalles, V., Lima, A. L. R., Kommareddy, I., Song, X., Wang, L., & Harris, N. L. (2022). Global Trends of Forest Loss Due to Fire From 2001 to 2019. *Frontiers in Remote Sensing*, 3. <https://doi.org/10.3389/frsen.2022.825190>

United States Geological Survey. (n.d.). *USGS Earth Explorer* [Dataset]. <https://earthexplorer.usgs.gov/>

USGS. (n.d.). *National Assessment of Coastal Vulnerability to Sea-Level Rise: Preliminary Results for the U.S. Atlantic Coast, USGS Open-File Report 99-593, Coastal Vulnerability Index*. Retrieved June 19, 2023, from <https://pubs.usgs.gov/of/1999/of99-593/pages/cvi.html>

Van Rijn, L. (2011). Coastal erosion and control. *Ocean & Coastal Management*, 54(12), 867–887. <https://doi.org/10.1016/j.ocecoaman.2011.05.004>

Vos, K., Splinter, K. D., Harley, M. D., Simmons, J. A., & Turner, I. (2019). CoastSat: A Google Earth Engine-enabled Python toolkit to extract shorelines from publicly available satellite imagery. *Environmental Modelling and Software*, 122, 104528. <https://doi.org/10.1016/j.envsoft.2019.104528>

World Bank. (n.d.). *World Bank Climate Change Knowledge Portal*. Retrieved June 19, 2023, from <https://climateknowledgeportal.worldbank.org/country/gambia/impacts-sea-level-rise>

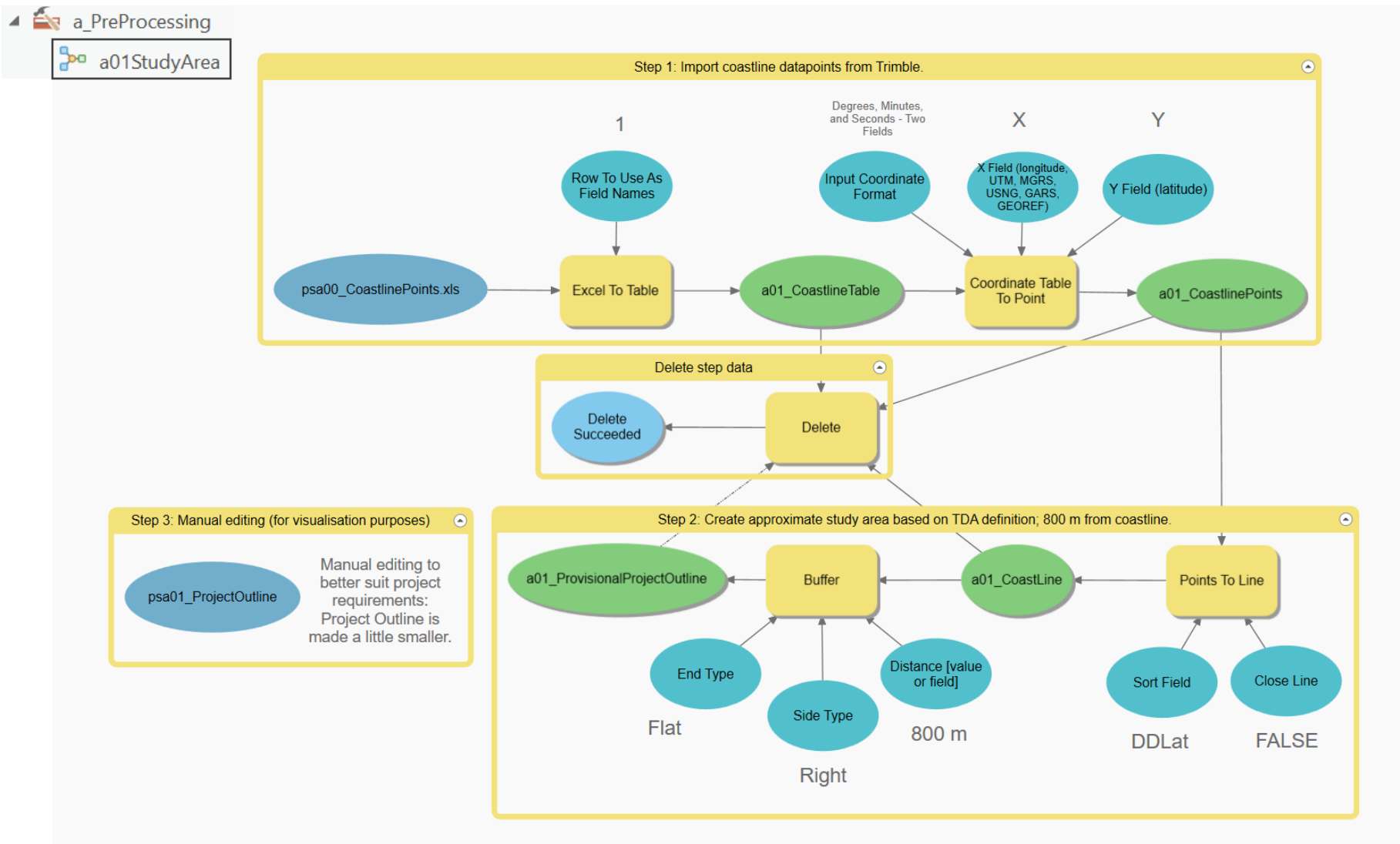
Wuebbles, D. J., Fahey, D. W., Hibbard, K., DeAngelo, B., Doherty, S. J., Hayhoe, K., Horton, R., Kossin, J. P., Taylor, P. C., Waple, A., & Yohe, C. (2017). *Executive summary. Climate Science Special Report: Fourth National Climate Assessment, Volume I*. <https://doi.org/10.7930/j0dj5ctg>

Zhang, K., Douglas, B. C., & Leatherman, S. P. (2004). Global Warming and Coastal Erosion. *Climatic Change*, 64(1/2), 41–58. <https://doi.org/10.1023/b:clim.0000024690.32682.48>

Annexes

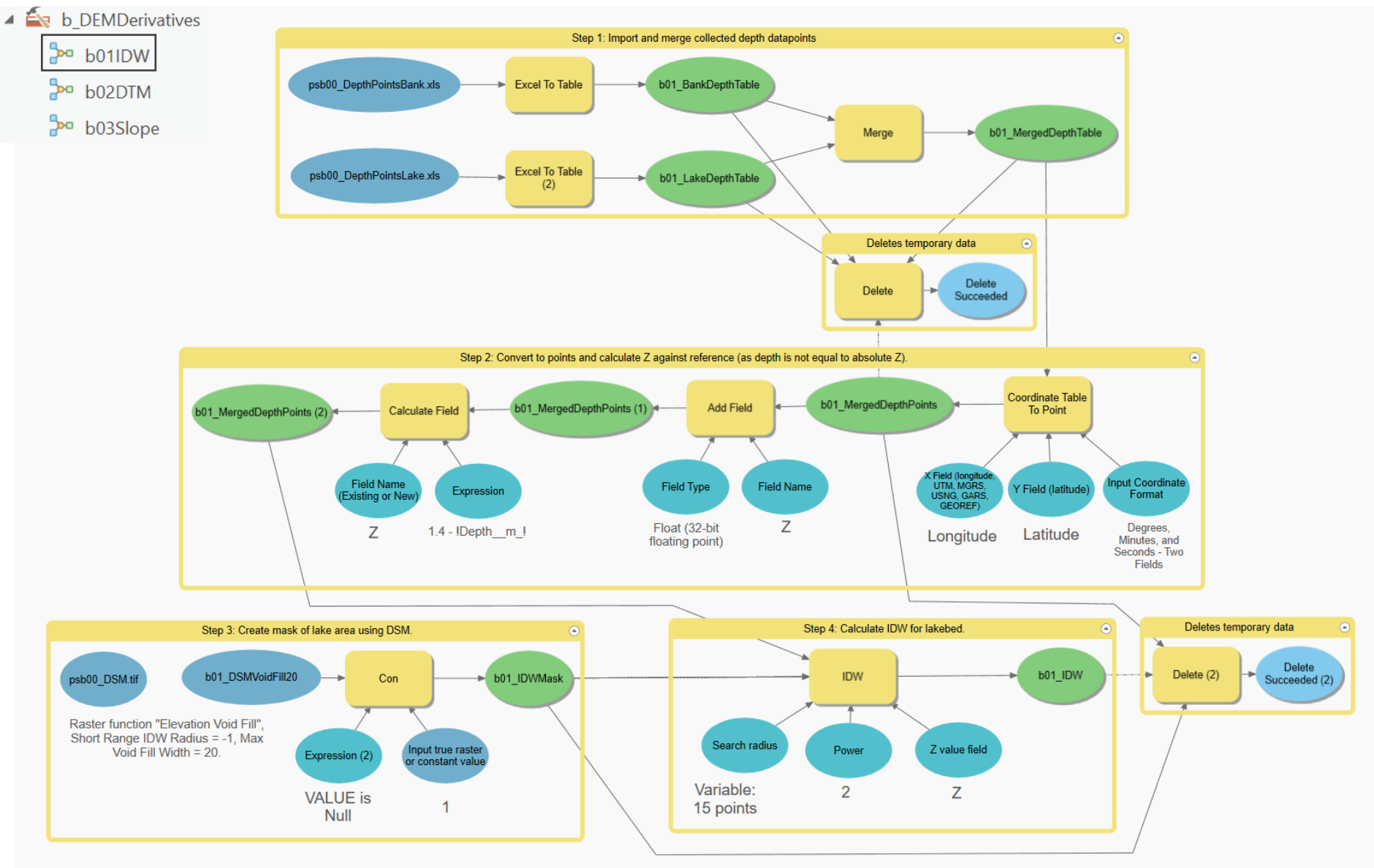
Annex I

ArcGIS Pro model builder: a_PreProcessing – a01StudyArea.

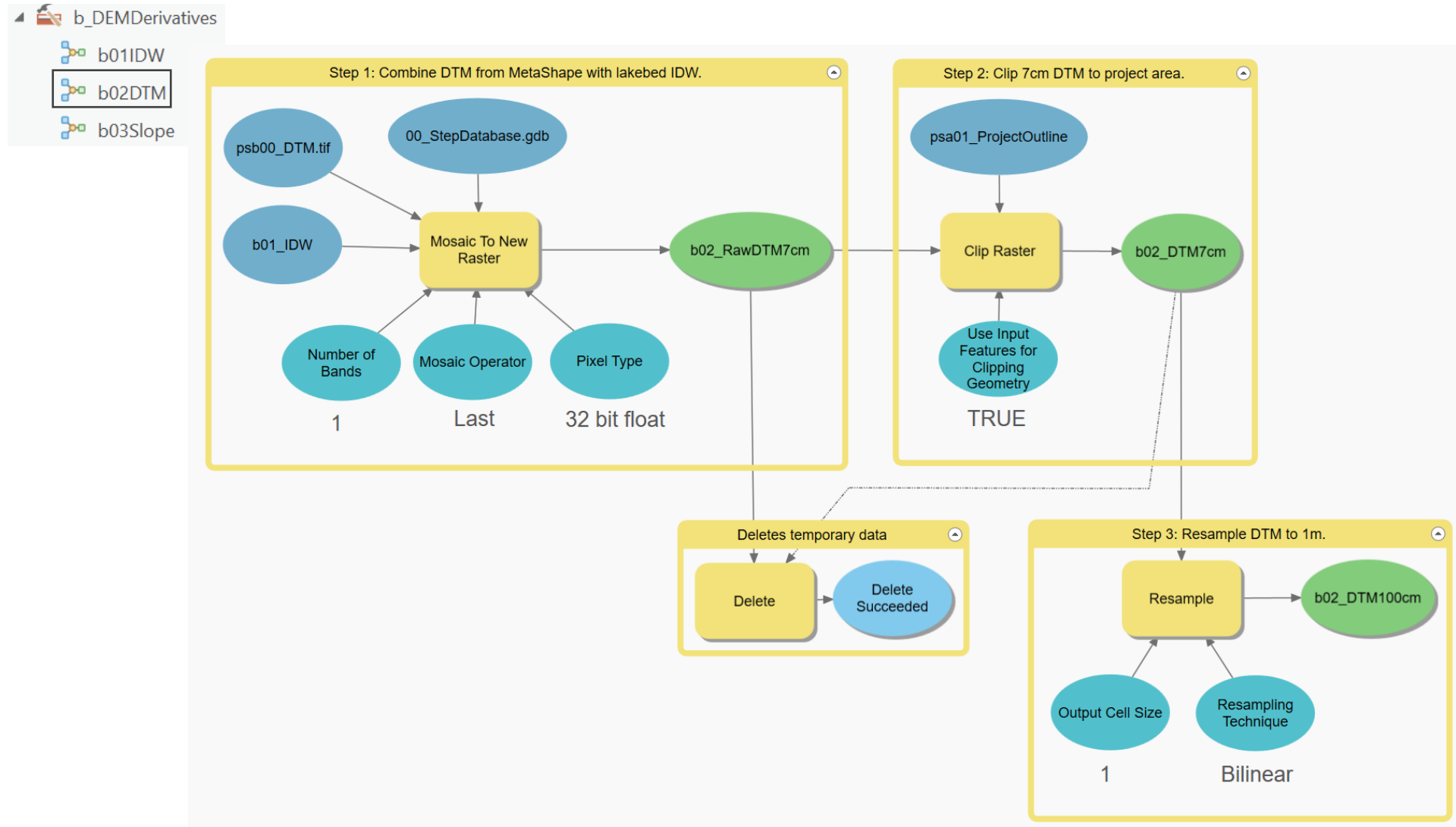


Annex II

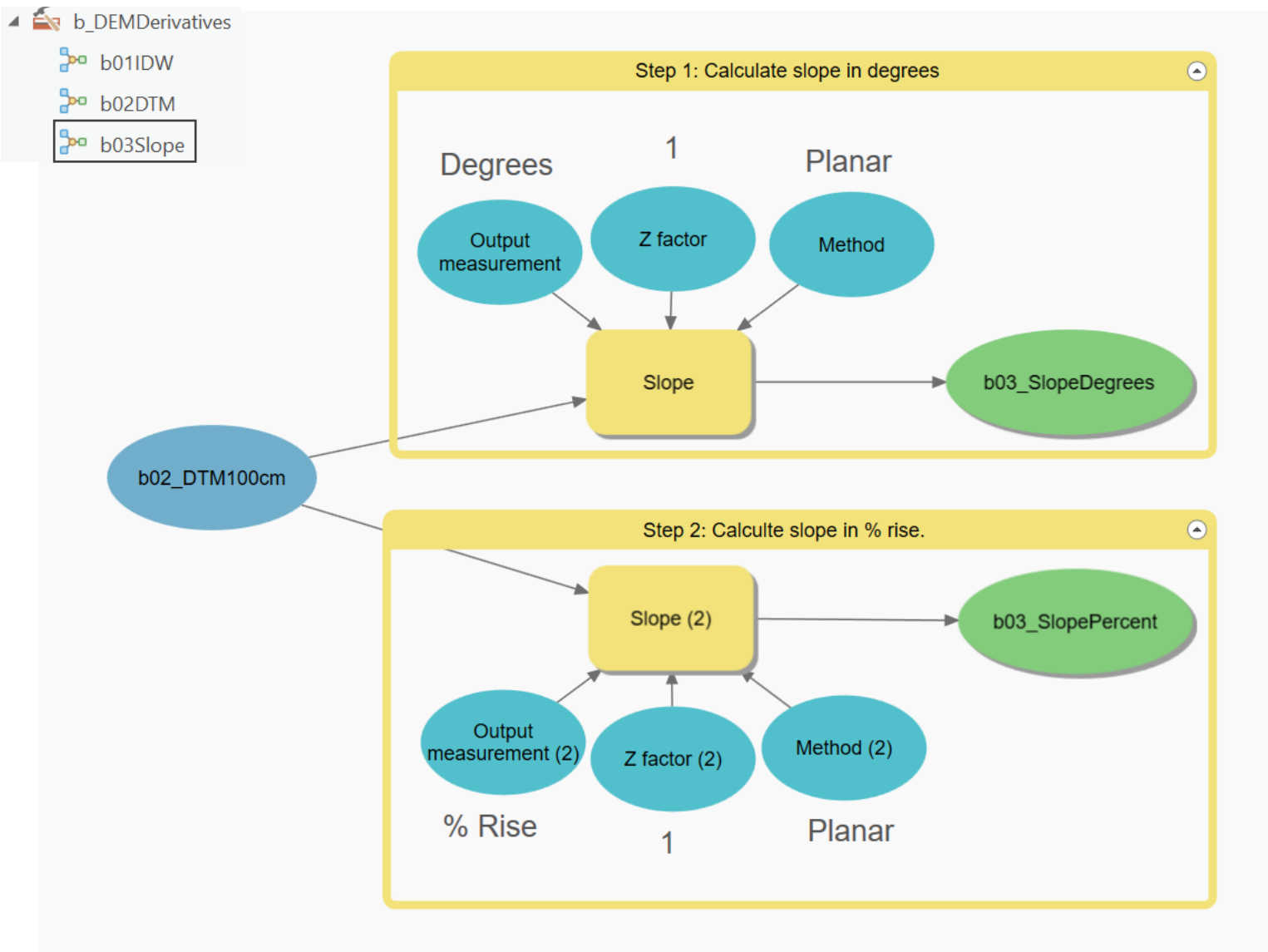
ArcGIS Pro model builder: b_DEMDerivatives – b01IDW



ArcGIS Pro model builder: b_DEMDerivatives – b02DTM

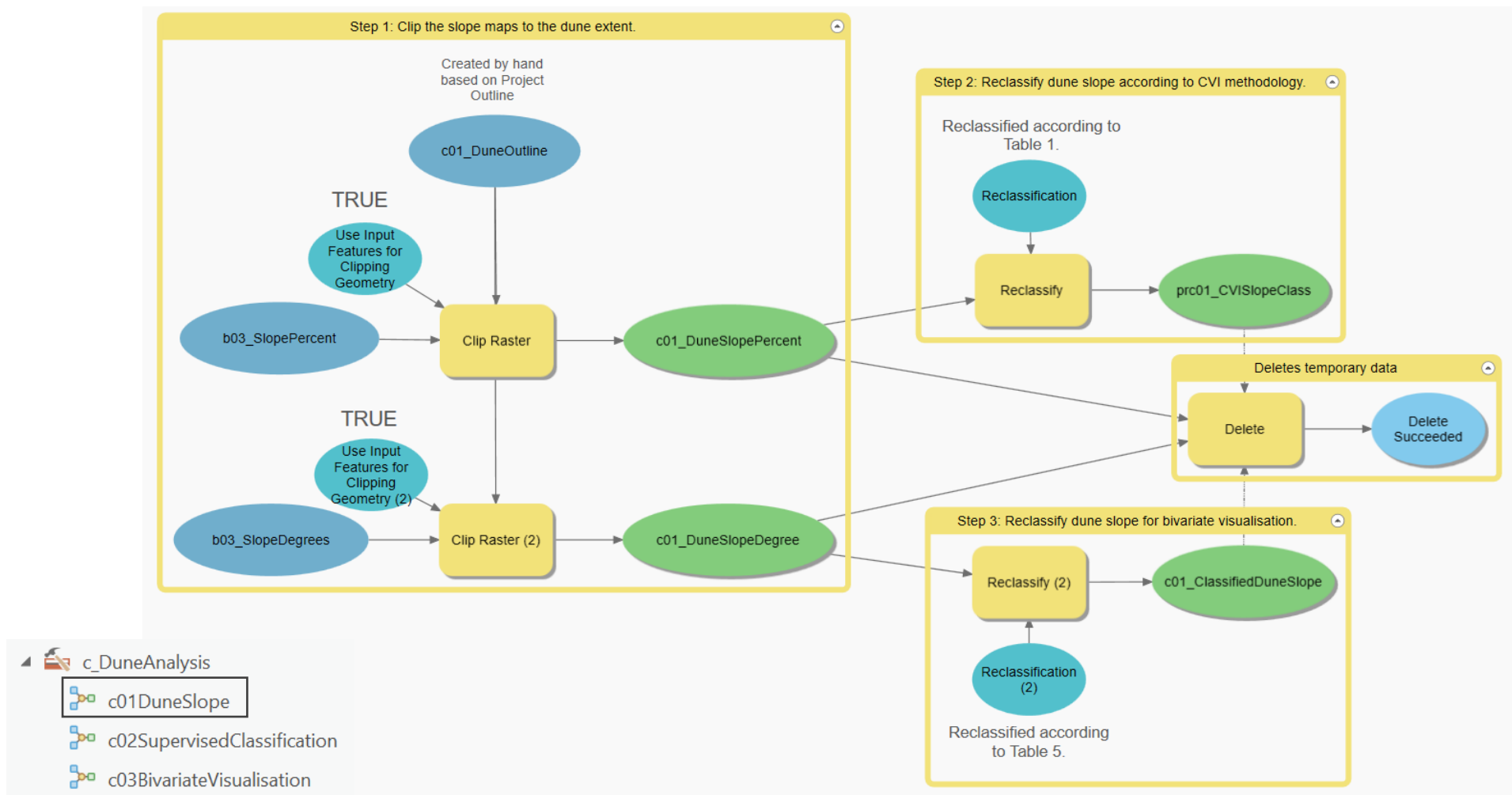


ArcGIS Pro model builder: b_DEMDerivatives – b02Slope

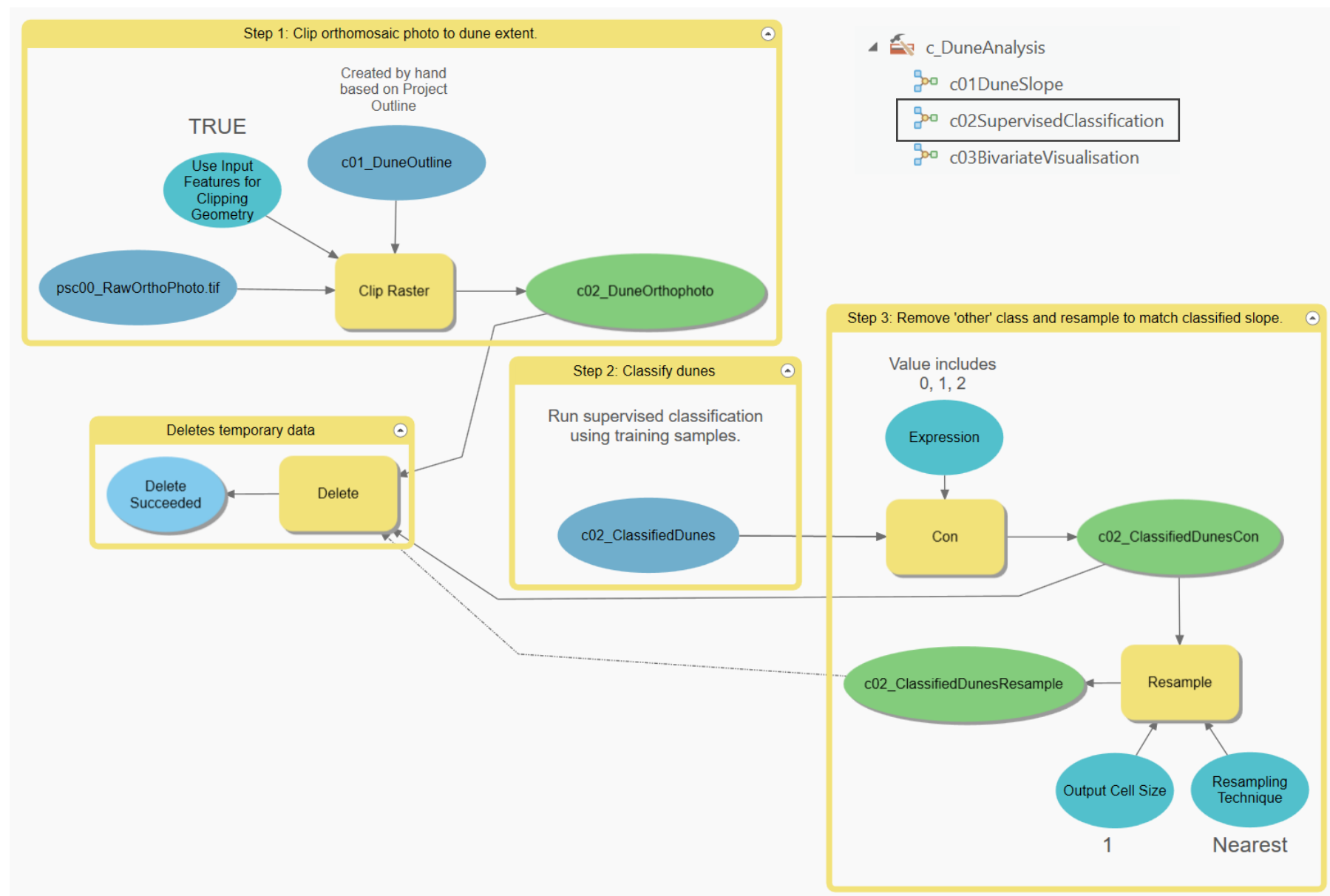


Annex III

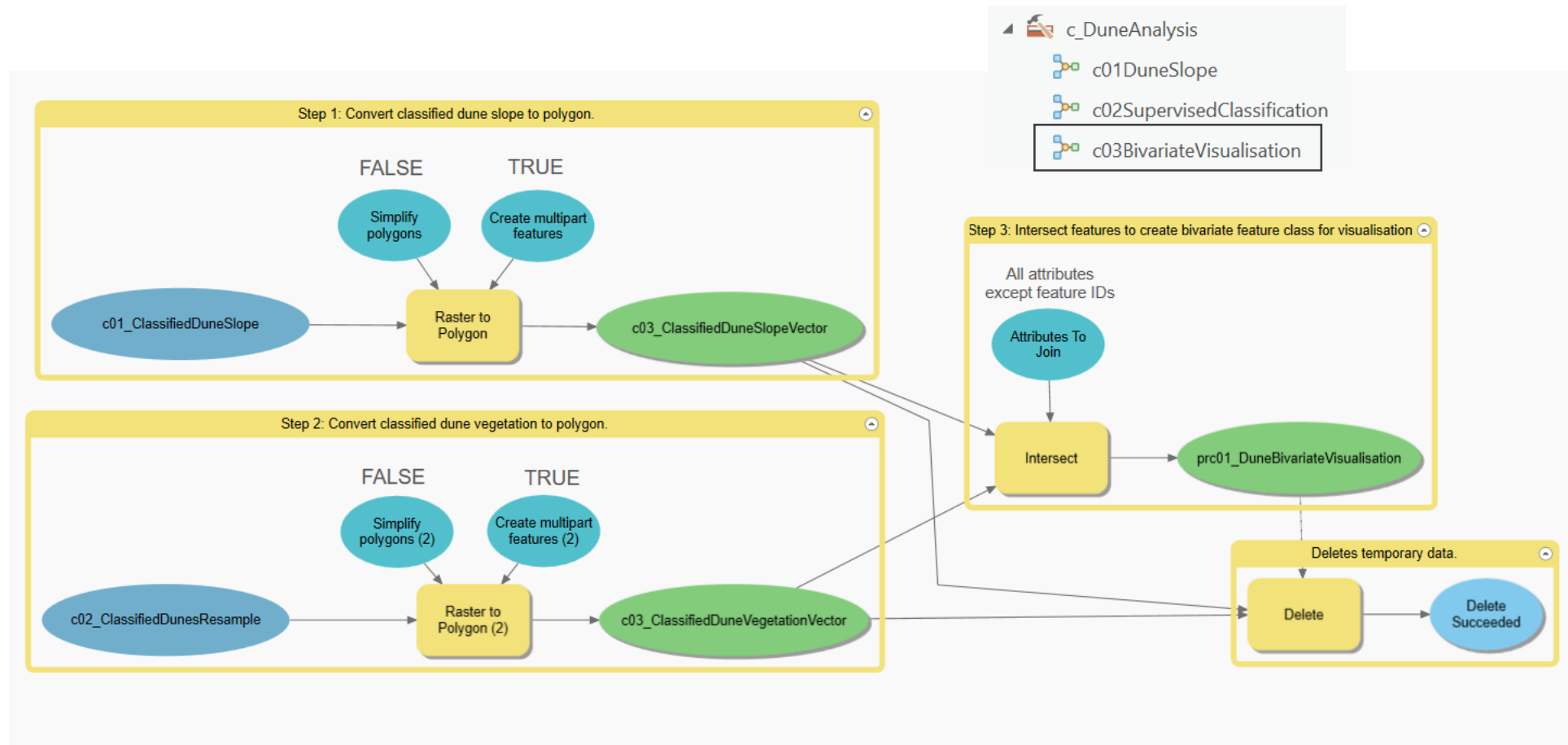
ArcGIS Pro model builder: c_DuneAnalysis – c01DuneSlope



ArcGIS Pro model builder: c_DuneAnalysis – c02SupervisedClassification

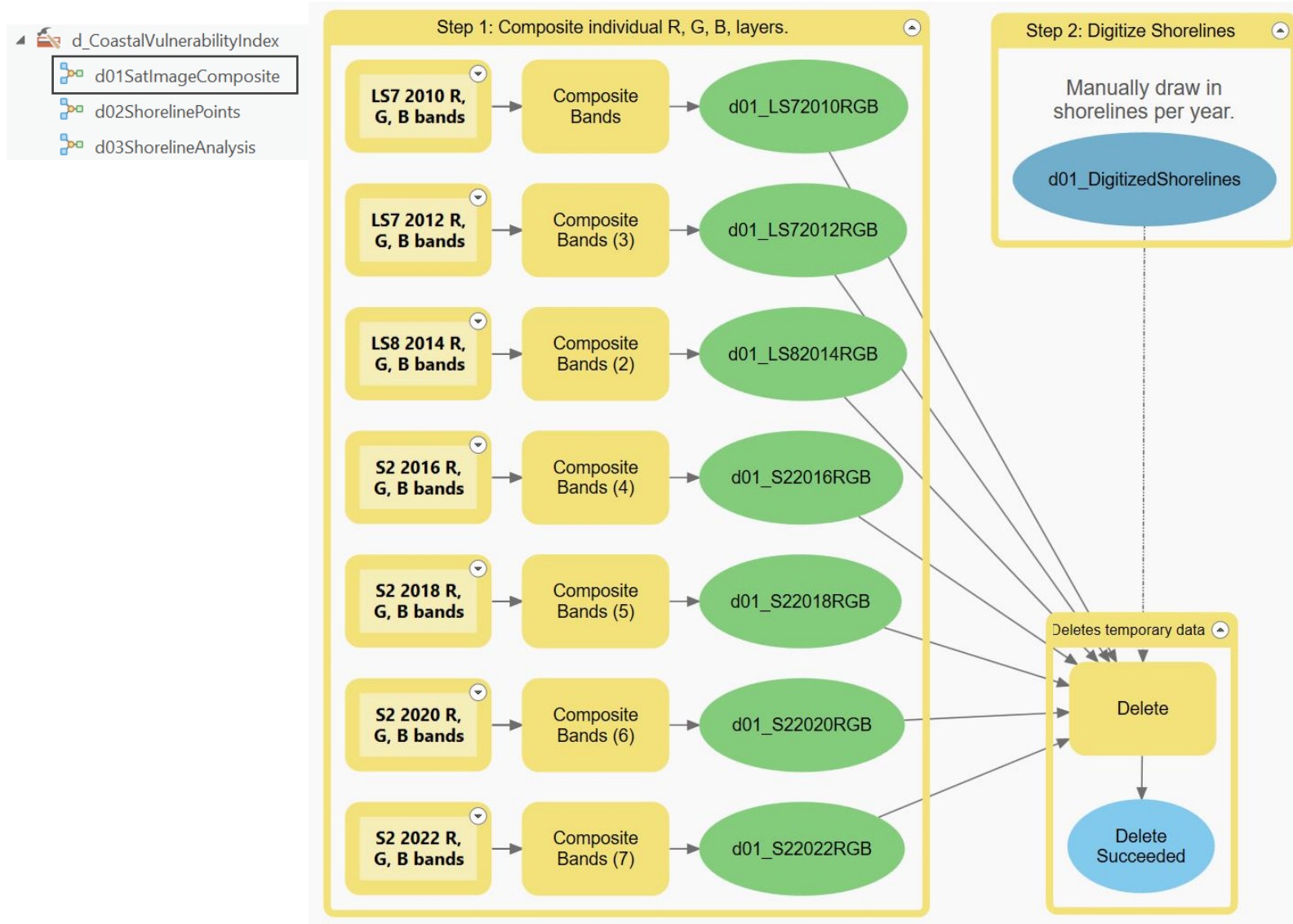


ArcGIS Pro model builder: c_DuneAnalysis – c03BivariateVisualisation

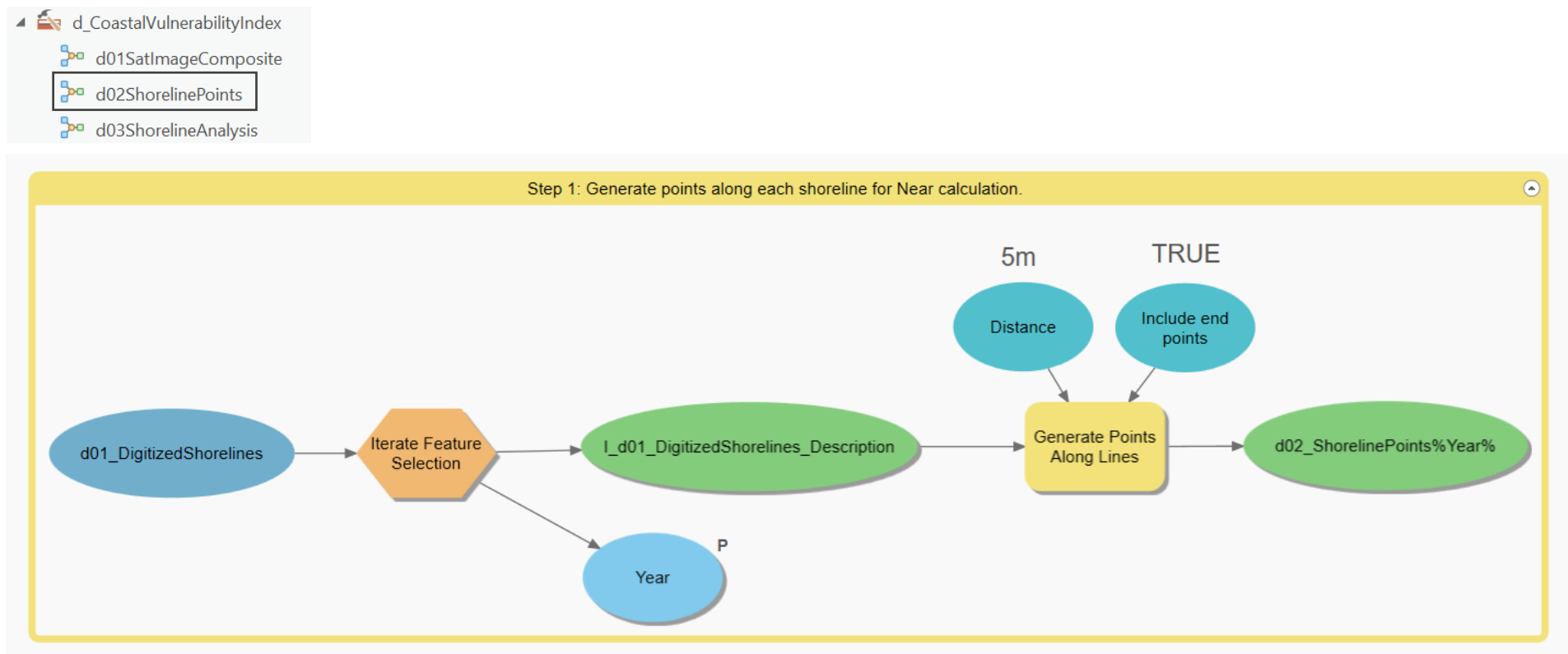


Annex IV

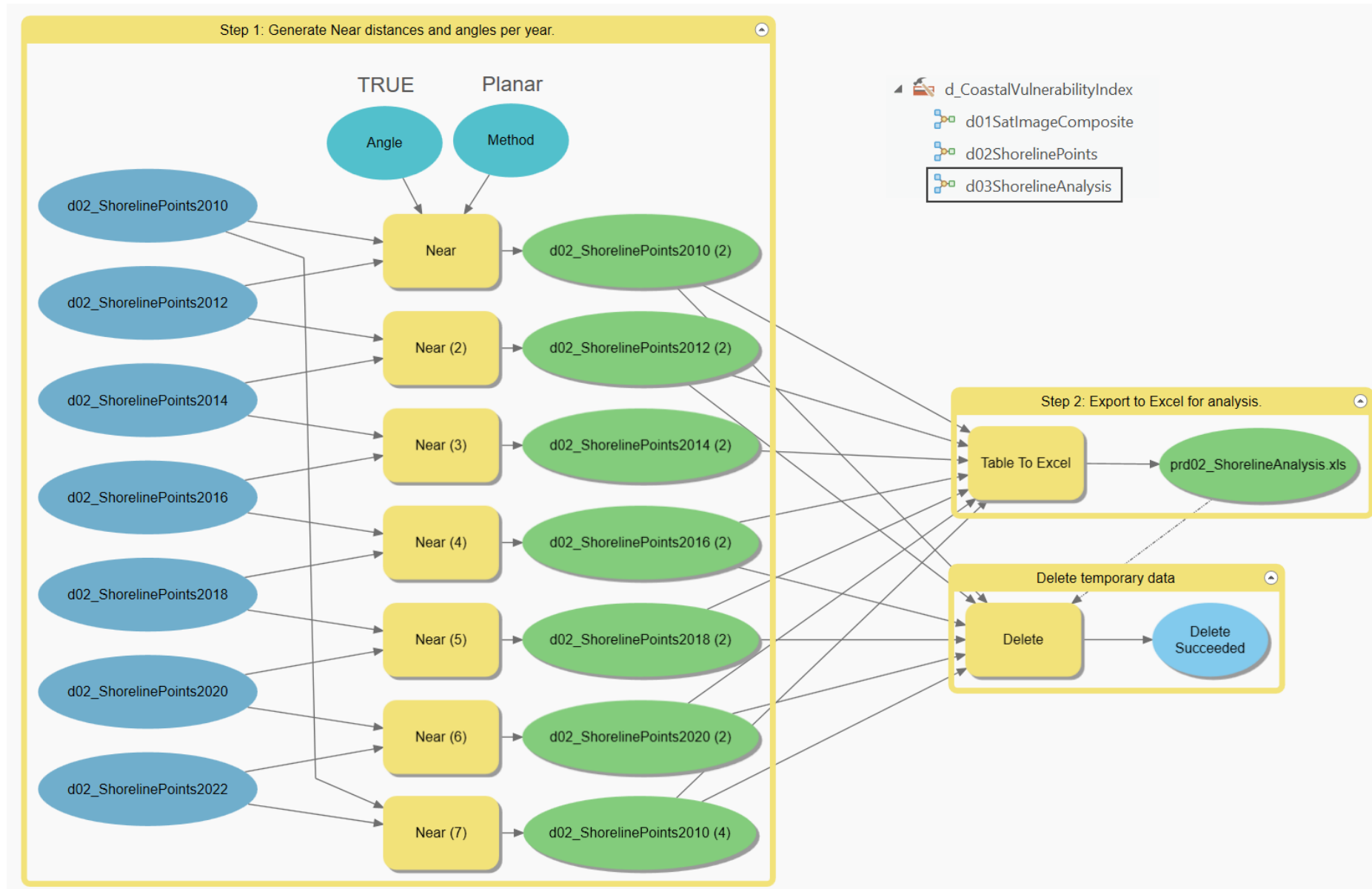
ArcGIS Pro model builder: d_CoastalVulnerabilityIndex – d01SatImageComposite



ArcGIS Pro model builder: d_CoastalVulnerabilityIndex – d02ShorelinePoints

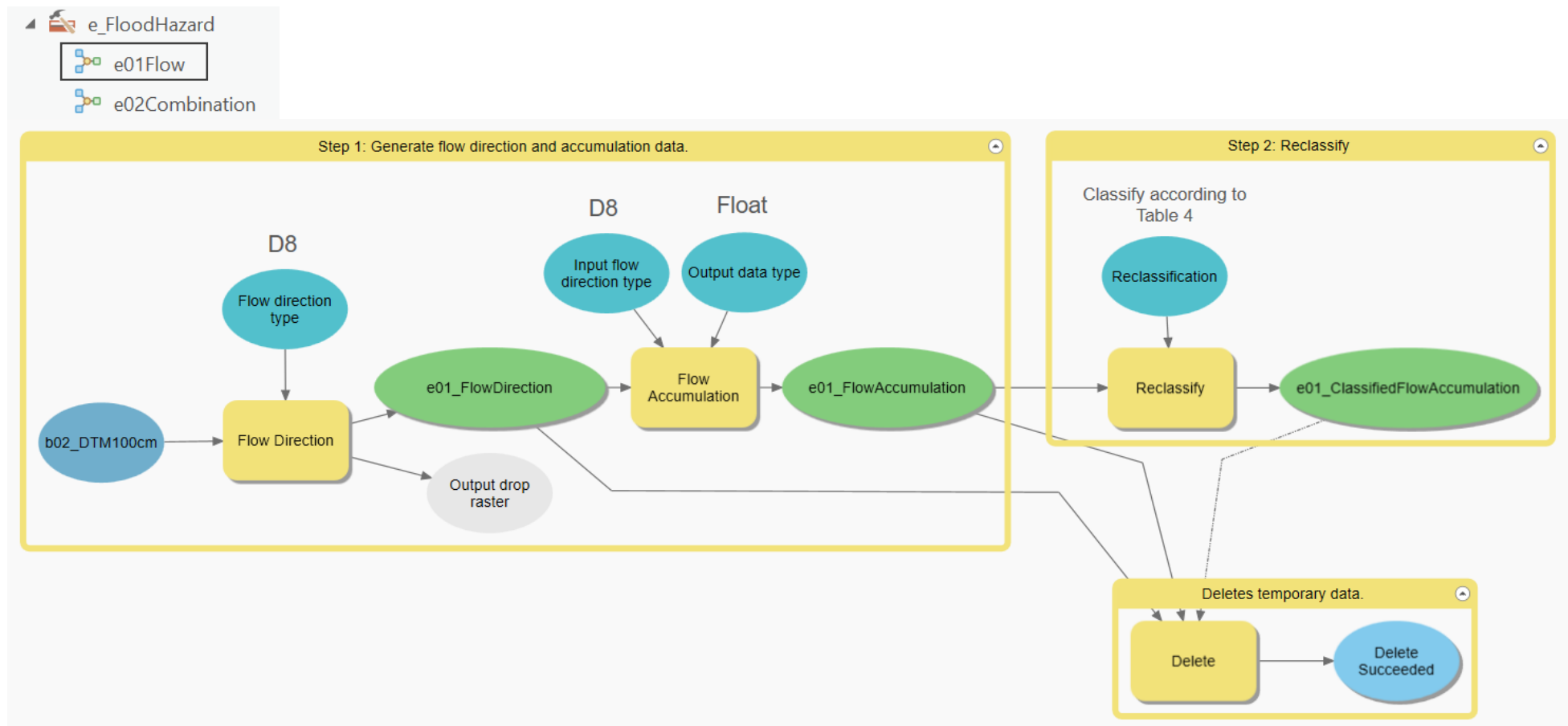


ArcGIS Pro model builder: d_CoastalVulnerabilityIndex – d02ShorelineAnalysis

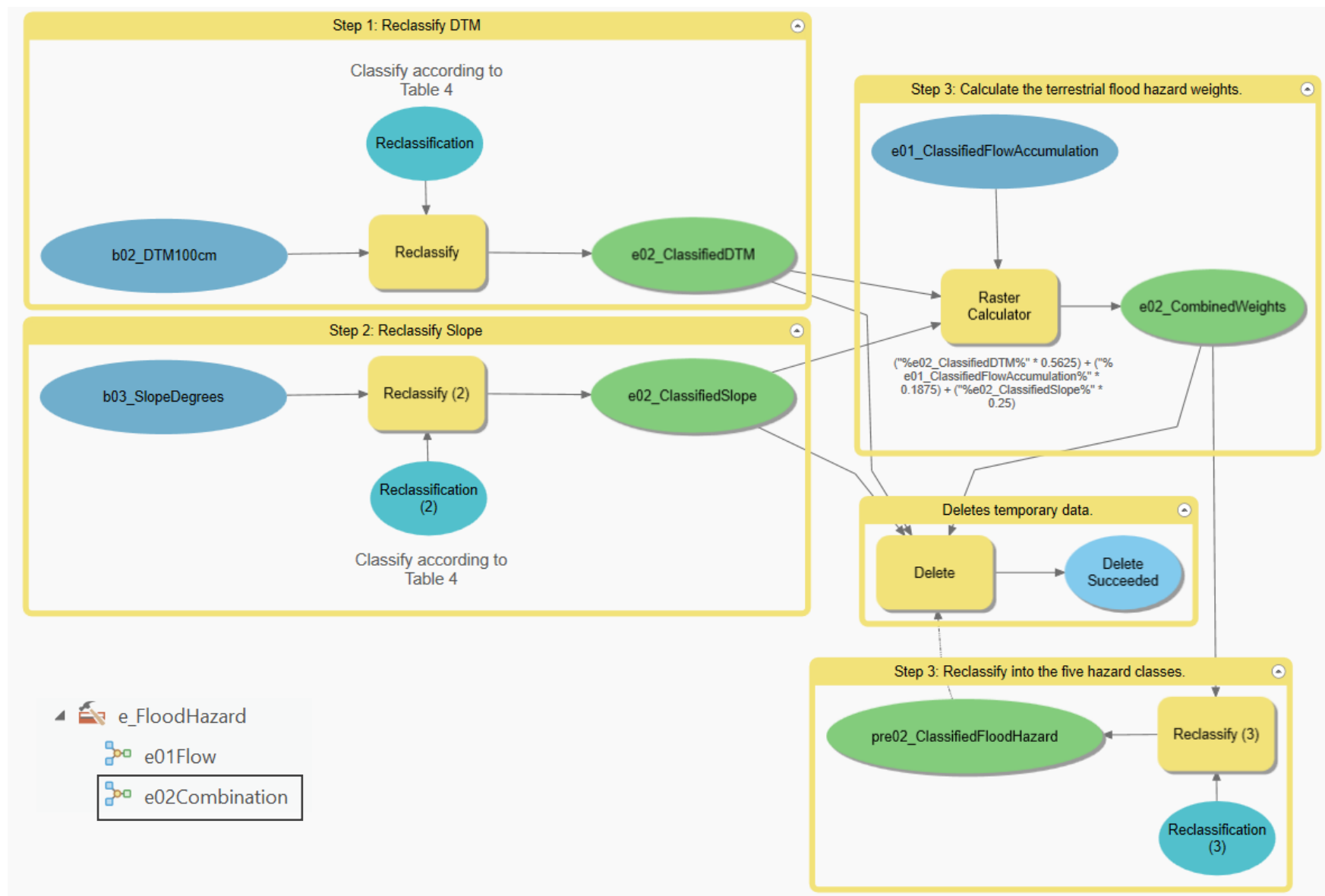


Annex V

ArcGIS Pro model builder: e_FloodHazard – e01Flow



ArcGIS Pro model builder: e_FloodHazard – e02Combination



Annex VI

Excerpt from Agisoft MetaShape processing report detailing accuracy/reliability of georeferenced UAV imagery based on GCPs collected.

Ground Control Points

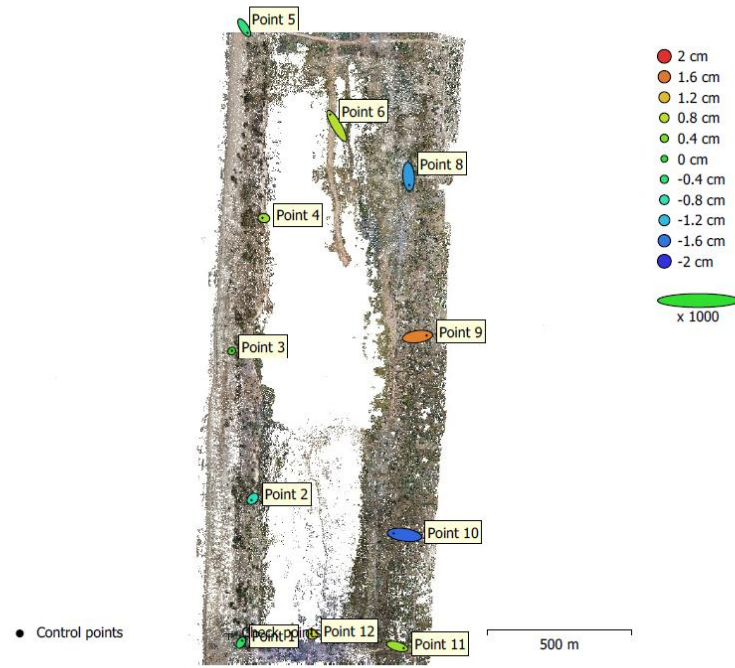


Fig. 5. GCP locations and error estimates.

Z error is represented by ellipse color. X,Y errors are represented by ellipse shape.

Estimated GCP locations are marked with a dot or crossing.

Count	X error (cm)	Y error (cm)	Z error (cm)	XY error (cm)	Total (cm)
11	3.61171	3.23437	0.969497	4.84826	4.94425

Table 5. Control points RMSE.

X - Easting, Y - Northing, Z - Altitude.

Label	X error (cm)	Y error (cm)	Z error (cm)	Total (cm)	Image (pix)
Point 1	0.862044	1.35803	-0.314791	1.63904	1.667 (25)
Point 2	-0.828875	-0.852713	-0.787198	1.42613	2.062 (16)
Point 3	0.207372	0.244376	0.111399	0.339312	1.345 (31)
Point 4	-0.982518	0.14158	0.61955	1.17014	1.671 (7)
Point 5	2.24532	-3.53358	-0.433269	4.20896	3.000 (6)
Point 6	-4.55123	7.8282	0.783682	9.08893	4.721 (10)
Point 8	0.459696	-5.94446	-1.38069	6.11999	1.901 (18)
Point 9	6.27969	0.822748	1.53291	6.51623	2.079 (16)
Point 10	-7.48157	1.02313	-1.69904	7.73999	3.525 (19)
Point 11	4.39438	-1.25199	0.624093	4.61168	2.208 (21)
Point 12	-0.60434	0.164693	0.943358	1.13238	1.302 (13)
Total	3.61171	3.23437	0.969497	4.94425	2.326

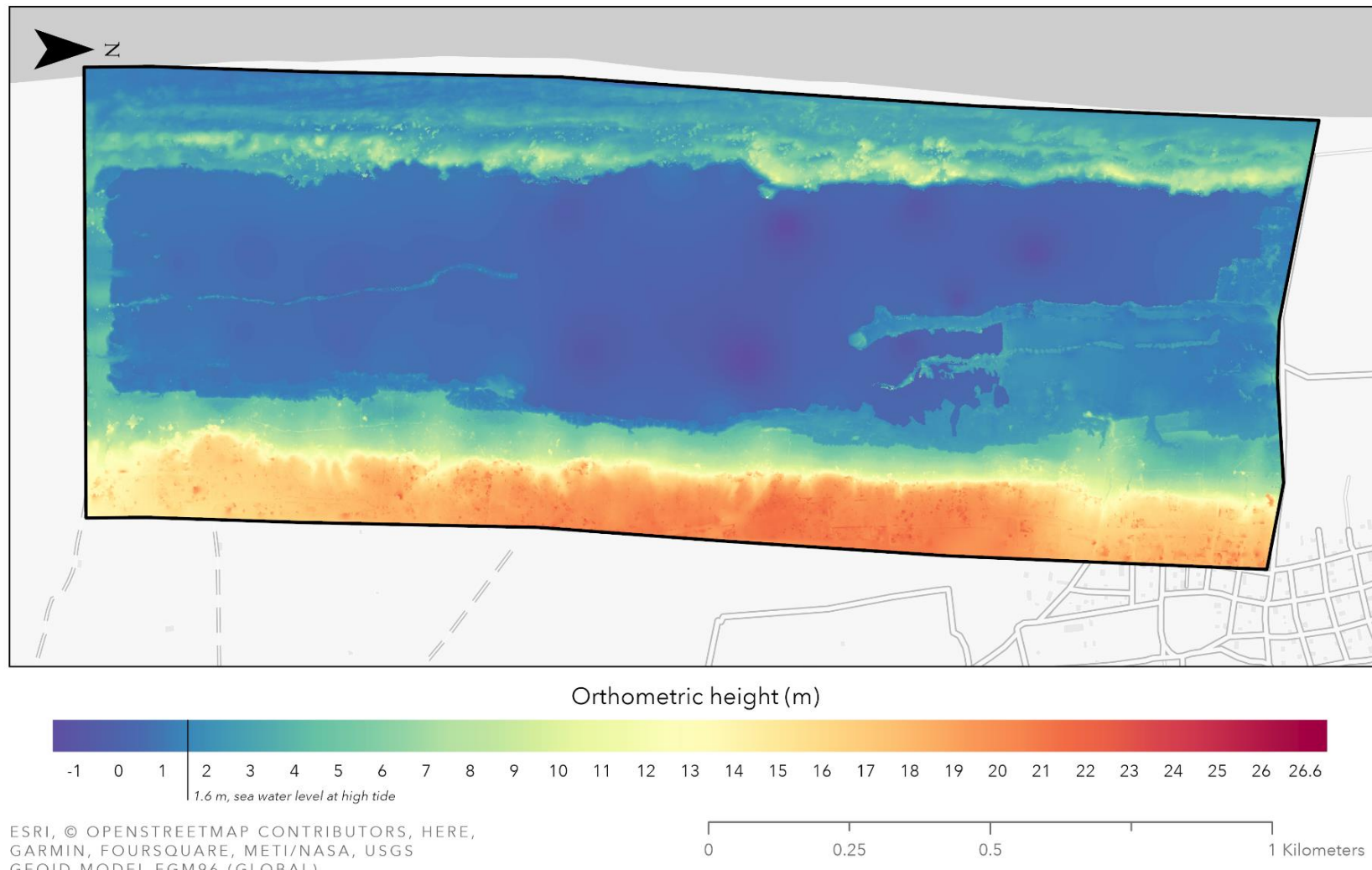
Table 6. Control points.

X - Easting, Y - Northing, Z - Altitude.

Annex VII

Visualisation of the Digital Terrain Model.

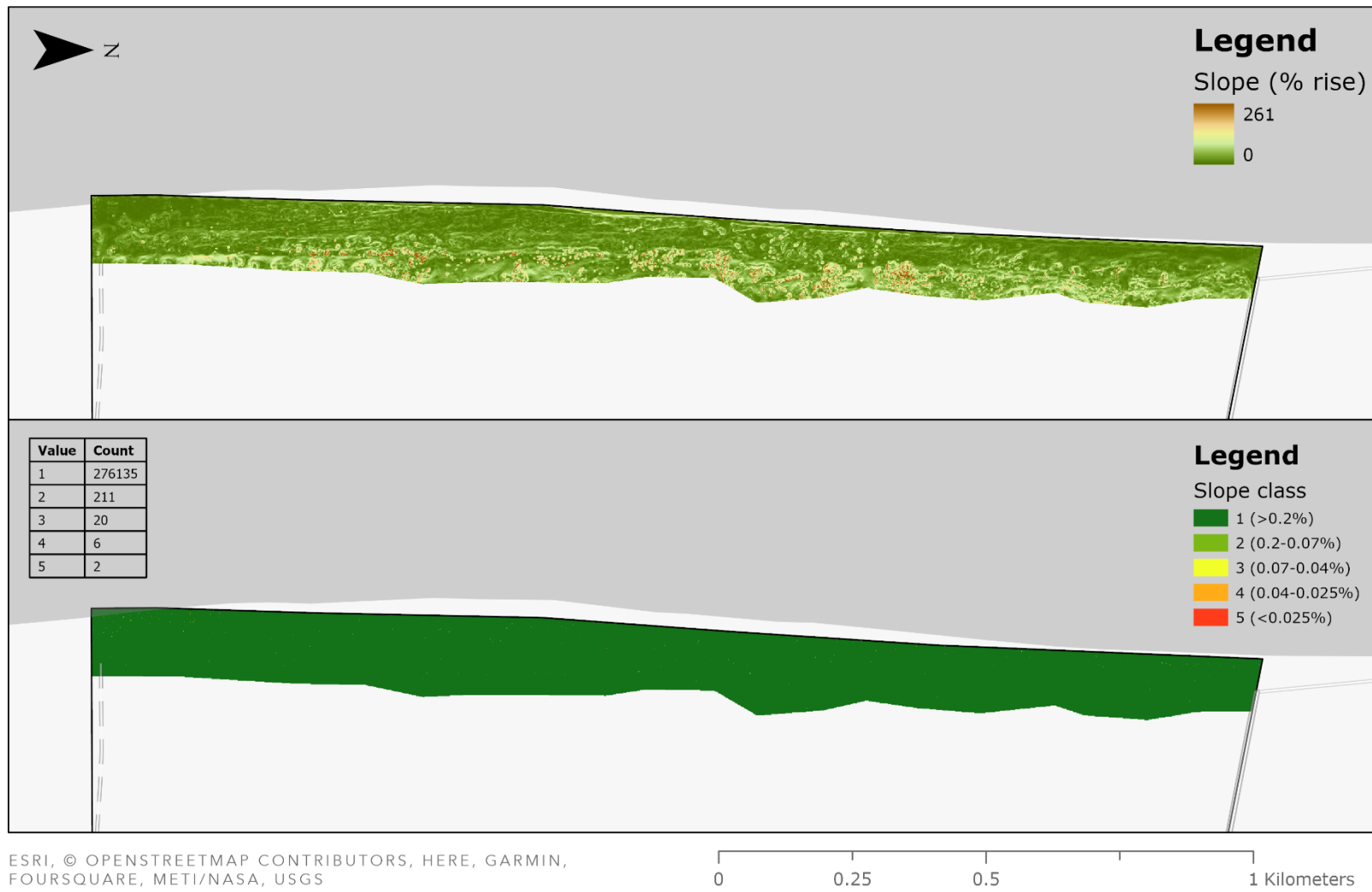
Digital Terrain Model of proposed project area



Annex VIII

Visualisation of the beach slope and classified slope.

Dune slope and slope class

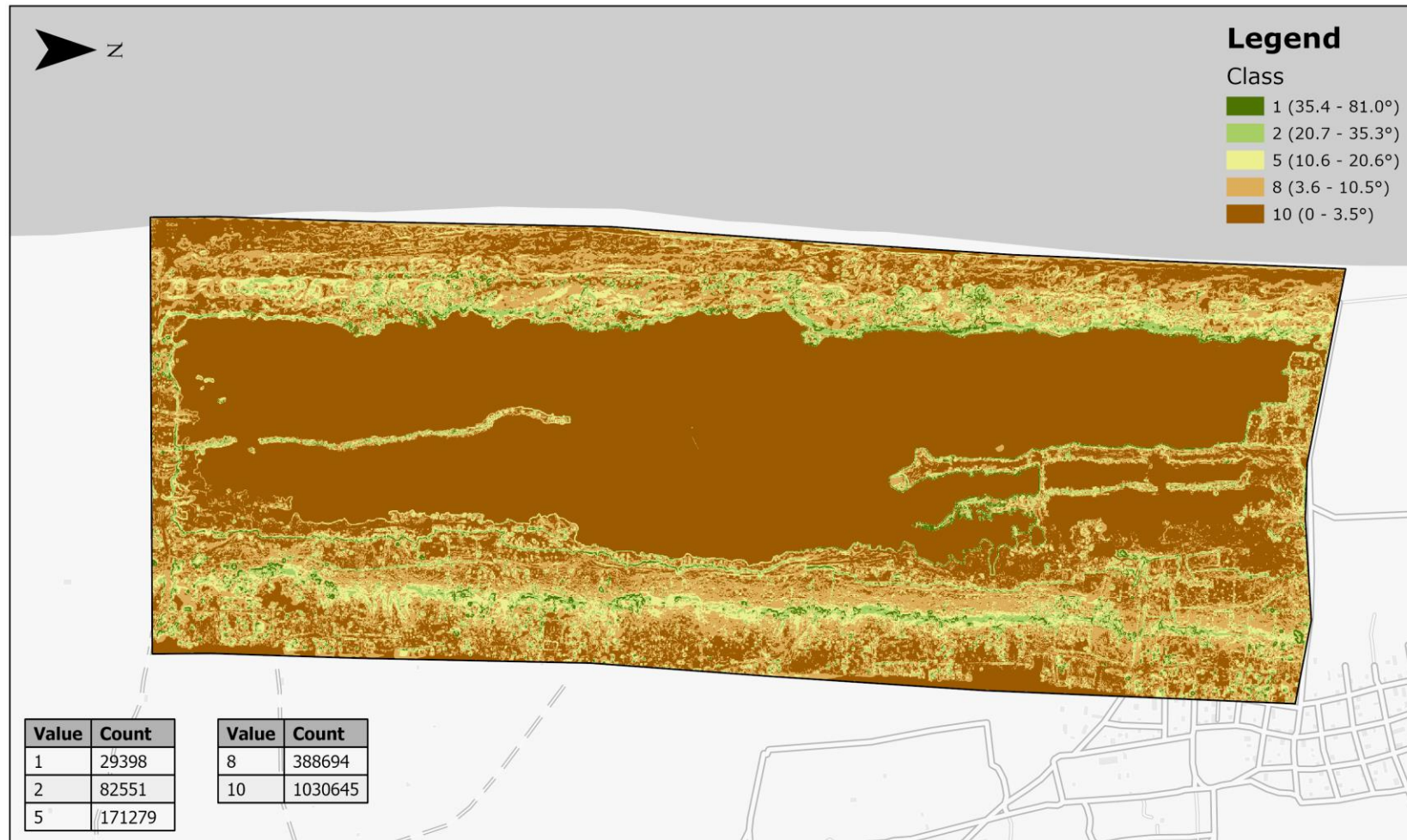


ESRI, © OPENSTREETMAP CONTRIBUTORS, HERE, GARMIN,
FOURSQUARE, METI/NASA, USGS
GEOID MODEL EGM96 (GLOBAL)

Annex IX

Visualisation of slope class.

Classified slope



ESRI, © OPENSTREETMAP CONTRIBUTORS, HERE, GARMIN,
FOURSQUARE, METI/NASA, USGS
GEOID MODEL EGM96 (GLOBAL)

0 0.25 0.5 1 Kilometers

Annex X

Visualisation of flow accumulation class.

Classified flow accumulation

